Seasonal hydrology explains interannual and seasonal variation in carbon and water exchange in a semiarid mature ponderosa pine forest in central Oregon

Christoph K. Thomas,[1,2] Beverly E. Law,[2] James Irvine,[2] Jonathan G. Martin,[2] J. Cory Pettijohn,[2] and Kent J. Davis[2]

Received 17 March 2009; revised 5 July 2009; accepted 30 July 2009; published 10 November 2009.

[1] We analyzed 7 years (2002–2008) of micrometeorological and concurrent biological observations of carbon and water fluxes at a mature ponderosa pine forest in central Oregon in a semiarid climate. We sought to evaluate the extent that gross primary productivity, net ecosystem exchange, ecosystem respiration, net primary productivity, net ecosystem productivity, tree transpiration, and evapotranspiration varied seasonally and interannually in this ecosystem subjected to varying periods and severity of droughts. To explain variation, we found it necessary to define seasons functionally within a hydroecological year rather than by fixed calendar dates. The interannual variability in growing season length was large (45 days), and the end date was more variable than the onset. Plant-available soil water was the main determinant of carbon fluxes. Spring evapotranspiration primarily used shallow water, whereas summer and fall evapotranspiration drew water from deeper in the soil profile. A multiyear drought (2001–2003) had a more severe and fundamentally different impact on carbon and water cycles than a single-year (2005) drought because of carryover effects in soil water and carbohydrate reserves in plant tissue. Calendar year–based analysis was inadequate to diagnose drought years in precipitation and ecosystem drought response. Extension of meteorological records back to 1982 showed that anomalies were coherent across the region and that the observations represented below-average precipitation and above-average temperatures coherent with a warm-phase Pacific Decadal Oscillation. The carbon sink of this seasonally water-limited ecosystem is anticipated to increase with increasing available soil water during the growing season.

Citation: Thomas, C. K., B. E. Law, J. Irvine, J. G. Martin, J. C. Pettijohn, and K. J. Davis (2009), Seasonal hydrology explains interannual and seasonal variation in carbon and water exchange in a semiarid mature ponderosa pine forest in central Oregon, *J. Geophys. Res.*, *114*, G04006, doi:10.1029/2009JG001010.

1. Introduction

[2] Valuable, novel insight into terrestrial carbon and water dynamics has been gained by studies either exceeding a 5 year observational threshold or synthesizing shorter-term observations at multiple locations up to continental and global scales [*Curtis et al.*, 2002, 2002; *Law et al.*, 2002; *Ma et al.*, 2007; *Reichstein et al.*, 2007; *Valentini et al.*, 2000]. These temporally or spatially aggregated data allow for identification of longer-term oscillations, anomalies and trends, and for assessment of their impact on and responses of terrestrial ecosystems. The response of ecosystem net balances of carbon and water exchange to a change in environmental drivers is of particular interest to further process understanding, improve its predictability to ongoing and future changes. This knowledge is also needed to meet societal challenges such as the impact of climate change on water availability and forest resources, and improving estimates of the terrestrial carbon sink to mitigate fossil fuel emissions.

[3] Although carbon and water exchange has been studied extensively in mesic ecosystems in humid climates with little or only sporadic drought stress, little attention has been given to semiarid, seasonally water-limited ecosystems. Semiarid or Mediterranean ecosystems are seasonally water limited each year and variability is caused by changes in duration, severity, and timing. Studies have been conducted in Mediterranean-type ecosystems in Europe and the western United States including grasslands and mixed oak savannas [*Ma et al.*, 2007; *Pereira et al.*, 2007; *Ryu et al.*, 2008; *Xu and Baldocchi*, 2004] and evergreen deciduous and coniferous forests [*Allard et al.*, 2008; *Grunzweig et al.*, 2003; *Maseyk et al.*, 2008; *Pereira et al.*, 2007; *Tirone et al.*, 2003] some of which span multiple years of observations. Even though the climate in central Oregon can be

[1]College of Oceanic and Atmospheric Sciences, Oregon State University, Corvallis, Oregon, USA.
[2]Department of Forest Ecosystems and Society, College of Forestry, Oregon State University, Corvallis, Oregon, USA.

0148-0227/09/2009JG001010$09.00

classified as Mediterranean, distinct differences exist: the mixed phase of wet season precipitation in form of rain and snow, the resultant persistent snowpack, and lower winter and annual air and soil temperatures. These differences are likely to have an impact on seasonal and annual assimilatory and respiratory processes. Ponderosa pine ecosystems are wide ranging in western North America [*Elias*, 1980] and exist in continental and mountainous habitats typically exposed to freezing winter temperatures and low annual precipitation primarily occurring between autumn and spring, and experience severe soil water and vapor pressure deficits in the summer dry season. The Pacific Northwest has been identified as a key ecoregion underrepresented in the continental AmeriFlux network [*Hargrove et al.*, 2003], and ponderosa pine forests account for approximately 22% of the western U.S. timberland [*Powell et al.*, 1993]. Mediterranean-type ecosystems including ponderosa pine stands were found to be significant net carbon sinks on annual time scales (see tables by *Allard et al.* [2008] and *Law et al.* [2002]) despite the seasonal limitations posed by the drought. However, sudden or gradual changes in precipitation and temperature patterns as a result of climate change or local climate oscillations may cause different responses in photosynthetic uptake and respiration losses of carbon dioxide. Those make it necessary to analyze the existing long-term data to better predict future responses. In particular, stressed ecosystems or shallow-rooted young forests may respond to subtle shifts in precipitation and temperature patterns much stronger than well-buffered systems with a high ecological inertia [*Irvine et al.*, 2004; *Schwarz et al.*, 2004].

[4] Net ecosystem exchange (NEE) is the difference between the ecosystem processes gross ecosystem productivity (GEP, photosynthetic assimilation) and ecosystem respiration (RE) including autotrophic and heterotrophic components. Carbon cycle analysis presents several challenges with respect to interannual and seasonal variability.

[5] 1. NEE is not an ecophysiological process, but a small residual between GEP and RE which may be an order of magnitude larger than NEE. Uncertainty estimates are therefore necessary separately for each component to test for significance of NEE in modeling studies, whereas uncertainty of observed NEE needs careful consideration of all its sources including instrumental errors.

[6] 2. Variability in NEE is the sum of changes in GEP and RE, which may lead to a nullified change of NEE in case of in-phase responses of its components [*Falge et al.*, 2002], or to an indirect, lagged response if changes in GEP and RE are out of phase or dominated by one component [*Falk et al.*, 2008; *Luyssaert et al.*, 2007; *Pereira et al.*, 2007; *Valentini et al.*, 2000].

[7] 3. The abiotic controls of photosynthesis and respiration well known for subdaily process scales such as light, temperature, water and substrate may not necessarily be key drivers on seasonal and longer time scales. Factors reported to impact ecosystem carbon balances are seasonal or annual air temperature [*Gough et al.*, 2008; *Lagergren et al.*, 2008; *Yuan et al.*, 2008], incident radiation [*Law et al.*, 2002; *Luyssaert et al.*, 2007], timing and changes in precipitation including droughts and associated water table fluctuations [*Krishnan et al.*, 2008; *Krishnan et al.*, 2006; *Reichstein et al.*, 2002; *Xu and Baldocchi*, 2004], seasonal precipitation and growing season length [*Allard et al.*, 2008; *Ma et al.*, 2007; *Xu and Baldocchi*, 2004], soil fertility and soil moisture [*Curtis et al.*, 2002; *Law et al.*, 2000], and succession [*Urbanski et al.*, 2007]. Changes in NEE may reflect a superposition of multiple factors.

[8] 4. The commonly applied flux partitioning algorithm of calculating GEP as residual between observed NEE and measured and modeled RE leads to a spurious self-correlation which can only be overcome if concurrent, independent estimates of either NEE or RE exist to derive an alternate GEP estimate [*Vickers et al.*, 2009b].

[9] Here we present 7 years of continuous micrometeorological and biological measurements of ecosystem carbon and water exchange in combination with detailed meteorological records over the period 2002–2008. We sought to evaluate the following hypotheses.

[10] 1. Growing season length controls carbon cycle dynamics; its onset is more variable than the end date and has a greater impact on annual NEE.

[11] 2. The carbon and water cycles are tightly coupled at seasonal, annual and interannual time scales, resulting in a conservative GEP/ET ratio, the denominator being ecosystem evapotranspiration. However, the impact of drought on the carbon and water cycles depends on drought duration; shallow, single-year droughts may increase net carbon uptake, whereas deep and multiyear droughts may be carbon neutral or decrease carbon uptake.

[12] 3. GEP and autotrophic respiration are coupled leading to a conservative ratio across seasons and years. In addition, we attempted to place the observation period into a larger interdecadal and regional context and to predict future ecosystem response in connection with a changing climate.

2. Materials and Methods

2.1. Study Site

[13] The site is a 90 year old mature ponderosa pine forest located east of the Cascades Mountains crest near Sisters, Oregon, USA, at an elevation of 1253 m (44.452 N, 121.557 W). This site is one of the Metolius cluster sites with different age and disturbance classes and part of the AmeriFlux network. The overstory is almost exclusively composed of ponderosa pine trees (*Pinus ponderosa* Doug. Ex P. Laws) with a few scattered incense cedars (*Calocedrus decurrens* (Torr.) Florin) and has a peak one-sided leaf area index (LAI) of 2.8 $m^2\ m^{-2}$. Tree height is relatively homogeneous at about 16 m above ground level (agl), mean tree density is approximately 325 trees ha^{-1} with a total base area of 24.4 $m^2\ ha^{-1}$ (2001) and 31.6 $m^2\ ha^{-1}$ (2006) [*Irvine et al.*, 2008]. The understory is sparse with an LAI of 0.2 $m^2\ m^{-2}$ and primarily composed of bitterbrush (*Purshia tridentata* (Push) DC. and Manzanita (*Arctostaphylos patula* Greene). Soils at the site are sandy (69%/24%/7% sand/silt/clay at 0–0.2 m depth and 66%/27%/7% at 0.2–0.5 m depth, and 54%/35%/11% at 0.5–1.0 m depth), freely draining with a soil depth of approximately 1.5 m [*Irvine et al.*, 2008; *Law et al.*, 2001b; *Schwarz et al.*, 2004]. A State of Oregon Water Supply Well Report from an irrigation water well in 2004 approximately 1.5 km South of the site indicated the following sequence: 0–0.9 m: topsoil gray; 0.9–3.4 m: clay or ash; 3.4–5.2 m: tuffstone; 5.2–195 m (maximum drilled depth):

varying basalt/tuff/red cinder. This well was not found to be productive, as only "weep water" was indicated in the report (http://apps2.wrd.state.or.us/apps/gw/well_log/Default.aspx). The fetch of the eddy covariance measurements extends in all directions for several kilometers into forest with similar and homogeneous characteristics except for the North where recent logging introduced a disturbance at a distance of approximately 500 m away from the tower. However, the flow is dominated by SW winds throughout the year.

[14] The climate can be described as Mediterranean (Csb) following Koeppen's climate classification with hot, dry summers and precipitation mostly falling in winter and spring as a combination of snow and rain when the site is in the polar front region. Temperate forests in this region of the Pacific Northwest are characterized primarily by transient soil moisture processes as a result of precipitation and temperature being out of phase, leading to soil water recharge occurring in the dormant reason [*Laio et al.*, 2001; *Waring and Running*, 2007].

2.2. Meteorological and Soil Hydrological Measurements

[15] Continuous observations of meteorological parameters such as mean wind speed (V_h) and direction (φ) (model R.M. Young Wind sentry, R.M. Young, Traverse City, MI, USA), air temperature (T_a) (models HMP45C, Vaisala, Helsinki, Finland in nonaspirated Gill radiation shield, and R.M. Young RTD-1000 temperature probe in aspirated R.M. Young radiation shield concurrently since 2006), relative humidity (RH) (model HMP45C, Vaisala, Helsinki, Finland in nonaspirated Gill radiation shield), global solar radiation (R_g) and net radiation (R_n) (model CNR-1, Kipp & Zonen, Delft, The Netherlands), photosynthetic photon flux density PPFD (models LI190SB, Licor, Lincoln, NE, USA replaced in 2006 by PARlite, Kipp & Zonen, Delft, The Netherlands) were carried out at the top of the main meteorological tower 32 m agl at a sampling rate of 10 s and aggregated into 30 min values during postprocessing.

[16] Precipitation was measured using a rain gauge (model TE525WS, Texas Electronics, Dallas, TX) on the tower at 32 m agl and additionally in small natural clearing next to the main tower using the same type of rain gauge equipped with a snowfall adapter during the winter and spring months. Sensors of snow depth and air temperature close to the ground ($T_{a,1.6m}$) were mounted on a 2 m tower in the same location. Horizontal separation between the two towers was approximately 10 m, and both were located in open spaces between trees characteristic for the ponderosa pine stands.

[17] Measurements of soil temperatures at multiple depths (thermocouples at 0.02, 0.04, 0.08, 0.16, 0.32 and 0.64 m) and surface soil volumetric water content (θ_s) integrating over the upper 0.3 m (model CS615, Campbell Sci., Logan, UT, USA) were continuously made adjacent to the 2 m tower and recorded as 30 min averages.

2.3. Atmospheric Carbon and Water Exchange

[18] Fluxes of momentum, carbon dioxide (F_c), temperature (sensible heat, H) and water vapor (latent heat, evapotranspiration, ET) were estimated from observations of the three dimensional wind vector and sonic temperature (model CSAT-3, Campbell Sci., Logan, UT) in combination with concentration measurements of carbon dioxide (CO_2) and water vapor (model Li-7500, Licor, Lincoln, NE, USA) sampled at 10 (2002 until 2005) or 20 Hz (2006 onward) at 33 m agl on the main meteorological tower using the eddy covariance (EC) technique. In this paper, NEE was defined as the sum of turbulent carbon dioxide flux F_c and change in storage term F_s evaluated from a vertical profile of mean CO_2 concentrations measurements (LI-820, Licor, Lincoln, NE, USA) measured at multiple heights (2002 and 2003: 1, 4, 30 m agl; 2004 and 2005: 1, 3, 6.2, 14.8, 33.5 m agl; from 2006 on: 0.3, 1, 3, 6, 10, 18, 33.5 m agl). The reader is referred to Appendix A for a detailed overview of the workflow (Figure A1) in EC data processing and details of the gap-filling techniques of NEE, ET and RE_{EC}.

[19] GEP was calculated as the difference between NEE and RE_{EC}. The symbol RE_{EC} was used for ecosystem respiration from the EC data as opposed to ecosystem respiration based on soil chamber, foliar and wood respiration described in section 2.4. The flux sign convention is positive away from the surface, so that GEP is negative, RE is positive, and positive NEE indicates a carbon source, and a negative NEE a carbon sink. Uncertainty in NEE was estimated using the maximum relative variability over the 7 years resulting from three different gap-filling approaches (see Appendix A).

2.4. Soil CO_2 Efflux and Alternate Ecosystem Respiration

[20] Soil CO_2 efflux (RE_{ch}) was routinely measured using 10 automated chambers each with a 0.21 m^2 of soil surface area [*Irvine and Law*, 2002]. Time series from individual chambers were recorded at a sampling interval of 60 min and combined into one spatial average. The hourly soil CO_2 efflux data were linearly interpolated to 30 min to synchronize with the atmospheric EC data. An average of 150 days of usable data was recorded from each automated chamber each year over the period 2002–2008. Monthly manual measurements of soil respiration (model Li-6400, Licor, Lincoln, NE, USA) from a spatially intensive array with 25 sampling locations were used to correct for biases in automated chamber location and technique. Further details of these observations and their analysis of seasonal and interannual variability can be found in the work by *Irvine et al.* [2008].

[21] Alternate ecosystem respiration was computed as RE = RE_{ch} + wood respiration + foliage respiration [*Law et al.*, 1999] concurrent to the data from the EC system (RE_{EC}). Here, we did not have seasonal foliage respiration (R_f) measurements, so phenological effects on R_f were not included. Respiration from coarse woody debris was also not included in the RE_{ch} estimates. Thus, RE_{ch} was likely to be an underestimate, albeit minor due to sparse mortality and logging residues, and the slow decomposition rates in this dry climate. Soil CO_2 efflux is the major component of ecosystem respiration at the study site and contributes about 70% to the total.

2.5. Sap Flux and Tree Transpiration

[22] Sap flux was measured using the heat dissipation technique [*Granier*, 1987] in the snow-free period between April and November each year. Twelve trees covering the

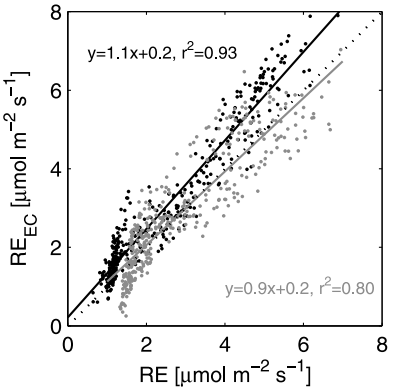

Figure 1. Comparing daily averages of ecosystem respiration from eddy covariance technique (RE_{EC}) to alternate ecosystem respiration based on soil chambers and foliage and wood respiration (RE) for the years 2002 (black) and 2005 (gray). Relative discrepancies between cumulative estimates were maximum for 2002 (17%) and minimum for 2005 (<1%). Solid lines are linear model equations and coefficient of determination (r^2).

range of tree diameters observed at the study site were instrumented with a combination of sap flux sensors installed in the outer conductive xylem and variable length heat dissipation sensors [*Jassal et al.*, 2007] to measure the radial sap velocity profile as a function of sapwood depth. The sap flux data from the sample set were then scaled to equivalent surface energy balance transpiration units (mm h^{-1}) using surveys of tree diameter distributions per *Irvine et al.* [2004].

2.6. Carbon Budget From Biological Measurements

[23] On a 1 ha plot, we measured tree and shrub dimensions, age and growth increment from wood cores, leaf area index (LAI), herbaceous plant biomass, coarse and fine woody detritus, and annual litter fall. On four 10 m radius subplots within each 100 × 100 m plot, structure measurements were made of incremental annual tree height with a laser ranging scope (models MapStar and Impulse 200, Laser Tech, Inc., Englewood, CO), and diameter at breast height (DBH, 1.37 m) on all trees >0.05 m DBH. The smaller trees were included in the shrub survey. Increment cores were taken from at least five trees per subplot to determine annual basal area increment and age. Shrub dimensions (length, width, height, diameter at shrub base) and herbaceous plant biomass were measured on 1–2 m radius microplots at each subplot center.

[24] Annual above and belowground wood productivity (ANPP, BNPP) were estimated from the increment cores and tree dimensions, and local allometric equations [*Law et al.*, 2001b, Table 3]. In addition, girth bands constructed from aluminum strapping and small extension springs were installed at 1.3 m agl (DBH) in early spring 2001 on 15 trees. These were measured using digital calipers every fall after seasonal radial increment was complete (typically in October). In summer 2002 an additional 69 trees were installed with girth bands and initial measurements made the following year, both sets of trees were measured through 2003 after which only the second group of trees was measured to the end of the period in this study. The data were used to generate a complete 7 year record of ANPP for those trees between 0.25 m and 0.40 m DBH (70% of the trees on site), minimizing any bias from a few small trees (average DBH 0.12 m) that had large relative basal increment, but contributed insubstantially to absolute changes in site annual basal increment. BNPP was estimated as the sum of coarse root increment and the product of fine root mass and fine root turnover. Coarse root increment was assumed to be 0.25 of wood production. Fine root mass was measured once in 2001 (see *Irvine et al.* [2007] for methodology) and coarsely scaled proportionally to soil respiration for the subsequent years, and site specific fine root turn over was taken from *Andersen et al.* [2008]. Net primary productivity (NPP) was then defined as NPP = ANPP + BNPP, where ANPP is aboveground net primary production (trees, shrubs, forbs and grasses), and BNPP is below ground net primary production (fine and coarse root growth). Heterotrophic respiration (R_h) was estimated from gap filled automated soil respiration data [from *Irvine et al.*, 2008] combined with monthly estimates of R_h fraction [from *Law et al.*, 2001a]. R_h fractions ranged between 0.50 and 0.54 in winter and spring (December through June) and 0.40 and 0.45 in summer and autumn (July through November). Net ecosystem production (NEP) was calculated as NEP = ANPP + BNPP − R_h.

3. Results and Discussion

3.1. Comparing Alternate Estimates of Ecosystem Respiration

[25] The concurrent, independent estimates of continuous RE_{EC} and RE were used to compare methods, estimate the uncertainty, and identify possible sources of error. Mean daily ecosystem respiration from the two independent methods compared well for all years with an annual maximum systematic difference in daily values of 40% (2006) and a significant correlation ($r^2 > 0.60$). Cumulative annual ecosystem respiration agreed well with a maximum difference of 17% in 2002 (Figure 1) used to define uncertainty in ecosystem respiration. The group of data with RE ≤ 2 μmol m^{-2} s^{-1} had a steeper slope compared to the data above and introduced some degree of nonlinearity. These data were primarily associated with colder winter months (Figure 3c) when RE was modeled using temperature response functions of its components. However, the cold season contributed very little to the annual carbon budget and the impact was therefore negligible. The difference between alternate estimates of gross ecosystem productivity of GEP = NEE-RE_{EC} and GEP_{alt} = NEE-RE were used to estimate uncertainty in annual budgets and were at a maximum of 13% in 2002.

3.2. Comparing Micrometeorological and Biometric Estimates of Net Carbon Exchange

[26] The 7 year average of biometric net primary productivity (NPP) was 466 ± 38 g C m^{-2} and agreed with that of NEE to within 1% (Figure 2). Biometric estimates of net ecosystem productivity (NEP), which include heterotrophic respiration (R_h), were considerably lower than NEE. The 7 year mean of NEP was 114 ± 52 g C m^{-2} (Table 2 and Figure 2). However, comparisons of alternate estimates of ecosystem respiration indicated robust agreement (Figure 1),

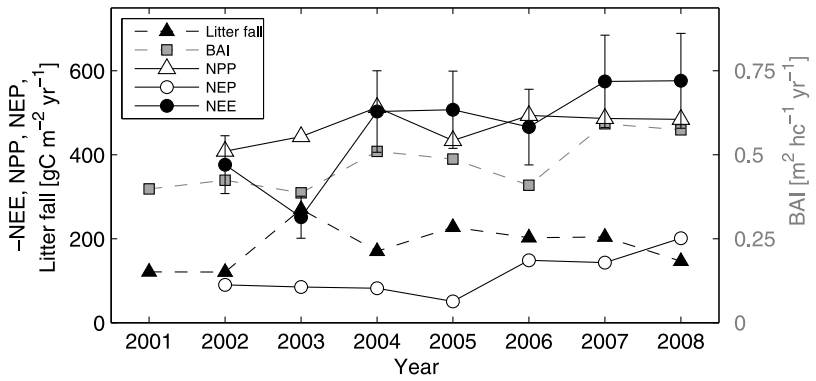

Figure 2. Time series plot of annual net ecosystem exchange (NEE) from micrometeorological, and litter fall, tree basal area increment (BAI), net primary productivity (NPP), and net ecosystem productivity (NEP) from biological measurements over the 7 year observation period at the mature ponderosa pine site in central Oregon. Bars depict uncertainty estimates.

which suggests that the often-found underestimation of nighttime respiration fluxes from micrometeorological methods was absent or negligible (see Appendix A). It is further unlikely to assume that both RE and RE_{EC} suffered from the same errors with similar magnitudes and temporal trends. Concerning biometric estimates of NEP, these values are largely driven by assumptions of belowground processes such as a fine root turnover, changes in soil carbon pools and soil heterotrophic respiration. Fine root turnover data and soil heterotrophic respiration fractions were quantified for this area [*Andersen et al.*, 2008; *Irvine et al.*, 2008], but further work is needed to determine their contribution to belowground carbon cycling in this dry ecosystem. Despite disagreement in magnitude, temporal trends of both NEE and NEP displayed low values early in the record with increasing values thereafter. Litter fall and NEE were mirror images where years of high NEE had less litter fall (Figure 2).

3.3. Seasonality and Growing Season Length: Calendar Versus Hydroecological Years

[27] Most studies investigating variability in carbon, water and energy exchange employ calendar years to delineate budgets and use the climatic definition of seasons with a fixed start and end date (winter: JFM, spring: AMJ, summer: JAS, autumn: OND). Although this selection may be justified for sites not experiencing significant interannual variations in climate variables and hydrological components while facilitating cross-site comparisons across biomes, it may not be appropriate for ecosystems sensitive to seasonal hydrology, e.g., caused by a summer drought as observed in the western United States. Calendar year–based seasonality alone does not statistically represent the cumulative soil water recharge occurring during the dormant period (from autumn through the subsequent spring) that has significant and well-documented impacts on ecosystem-scale water limitations of the subsequent growing season [*Botter et al.*, 2008; *Daly et al.*, 2004a, 2004b; *Porporato et al.*, 2001; *Rodriguez-Iturbe and Porporato*, 2004]. Models typically assume that incident radiation is the primary control on vegetation productivity (e.g., light use efficiency models), and therefore, also use calendar years. One may hypothesize that ecosystems experiencing limitations due to exhaustion of one or multiple resources are more sensitive and vulnerable to subtle changes than well-buffered ecosystems with plentiful resources throughout the year. Analysis based on the calendar year's fixed seasons may therefore mask important responses to subtle changes in site environmental conditions of stressed ecosystems.

[28] The ponderosa pine ecosystem experiences summer drought almost every year caused by the strong seasonality in precipitation, air and soil temperatures, and resultant snowpack (Figures 4a–4d), which leads to an exhaustion of surface soil moisture, reduction of evapotranspiration and tree transpiration (Figures 3d and 4e), a decrease in the ratio of actual to potential ET (Figure 4f), and an increase in vapor pressure deficit (Figure 3e), and a subsequent reduction of GEP, ecosystem respiration, and NEE (Figures 3a–3c). Interannual changes in duration, severity, and timing of the drought are caused by the variability of the above mentioned environmental drivers causing the variability in ecosystem carbon and water cycles. We here introduce the concept of a hydroecological year (HEY) for the analysis of carbon and water exchange and their environmental drivers to better account for seasonal and interannual variability. The length of a hydroecological year equals 365 days starting 21 November. This date reflects a break point in the site climate when daily mean air temperatures dropped below freezing within a few days consistently across the observation period. Surface soil temperatures ($T_{s,02cm}$) lagged by 3–4 days. This break point was chosen to represents the onset of the dormant period with minimal plant activity as water in liquid phase is mostly unavailable and physiological processes are severely limited by the low temperatures. In addition, a continuous variable such as air temperature lent itself better to the determination of a break point than a noncontinuous variable such as precipitation. Alternate start dates of the hydroecological year chosen after the conventional water year (1 October) or the mean onset of autumnal rains (28 November) caused annual carbon and water fluxes to be different by less than 3%. Seasons within a hydroecological year were delineated flexibly depending on the timing of ecologically meaningful events in the site hydrology detailed in section 3.3.1. The

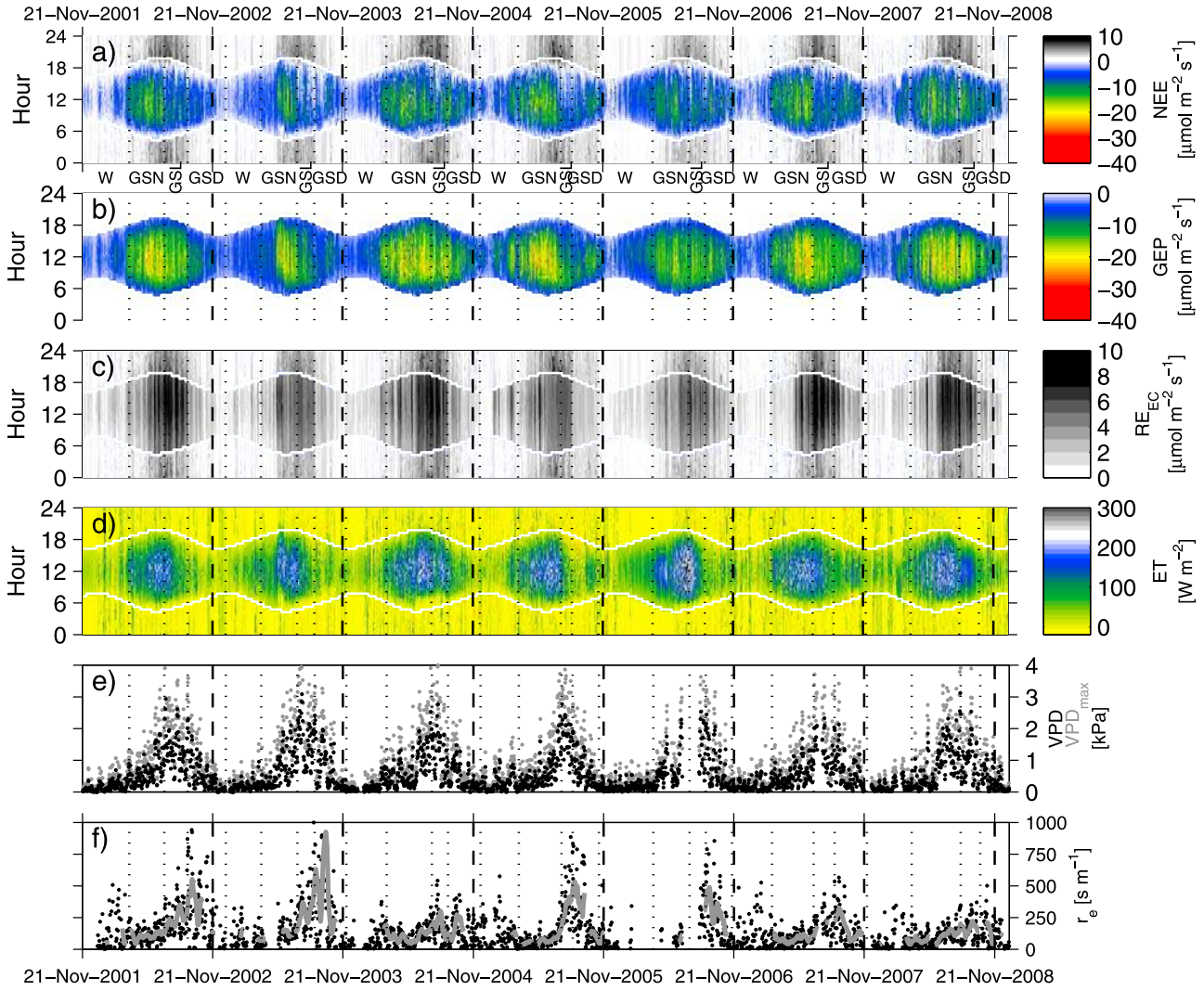

Figure 3. Carbon and water exchange, flux-derived variables, and associated meteorological variables observed in the ponderosa pine forest in central Oregon: (a) net ecosystem exchange (NEE), (b) gross ecosystem productivity (GEP), (c) ecosystem respiration (RE_{EC}), (d) evapotranspiration (ET) in 30 min resolution calculated from above-canopy eddy covariance measurements, (e) daily aggregates of mean (VPD) and maximum (VPD_{max}) vapor pressure deficit, and (f) maximum daytime ecosystem resistance (r_e) derived from a Penman-Monteith model (see Appendix B). Gray line in Figure 3f is 2 week running average. Vertical lines mark hydroecological years (bold dashed) and their seasons (light dotted) of winter (W), growing season nonlimited (GSN), growing season limited (GSL), and growing season drought (GSD). See sections 3.3 and 3.3.1 for details.

concept of using a start date different from 1 January of the calendar year is not entirely novel and has been used for the definition of "ecological years" at a deciduous site based on the timing of leaf on/off cycles [*Urbanski et al.*, 2007]. However, the authors of that study used fixed seasons and did not allow for variation between years. Hydrologists typically examine water budgets across years using water years defined from 1 October through 30 September to better account for variability in winter precipitation, but we have refined that to represent seasonal ecosystem functioning. Furthermore, simplified probabilistic ecohydrologic models of soil moisture dynamics inherently ignore calendar year divisions as they are typically forced by the stochastic nature of precipitation [*Rodriguez-Iturbe and Porporato*, 2004].

3.3.1. Defining Ecologically Meaningful Seasonality Within a Hydroecological Year

[29] We delineated four functional seasons within a hydroecological year with regard to the site hydrology.

[30] 1. The physical significance of winter (W) is given by the hydrological recharge leading to nonwater limited conditions for plants. Despite these water resources, the trees are primarily dormant due to the low air and soil temperatures in concert with low light intensities (Figures 3a–3d, 4a, and 4b). Surface soil temperatures are close to 0°C depending on snow cover (Figures 4b and 4c). The start of the hydroecological winter is defined by surface soil moisture $\theta_s \geq 0.3$ m^3 m^{-3} toward the end of the calendar year (Figures 4d and 5b) caused by the onset of autumnal rains. The threshold of 0.3 m^3 m^{-3} is the vegetation stress point θ^* below which soil

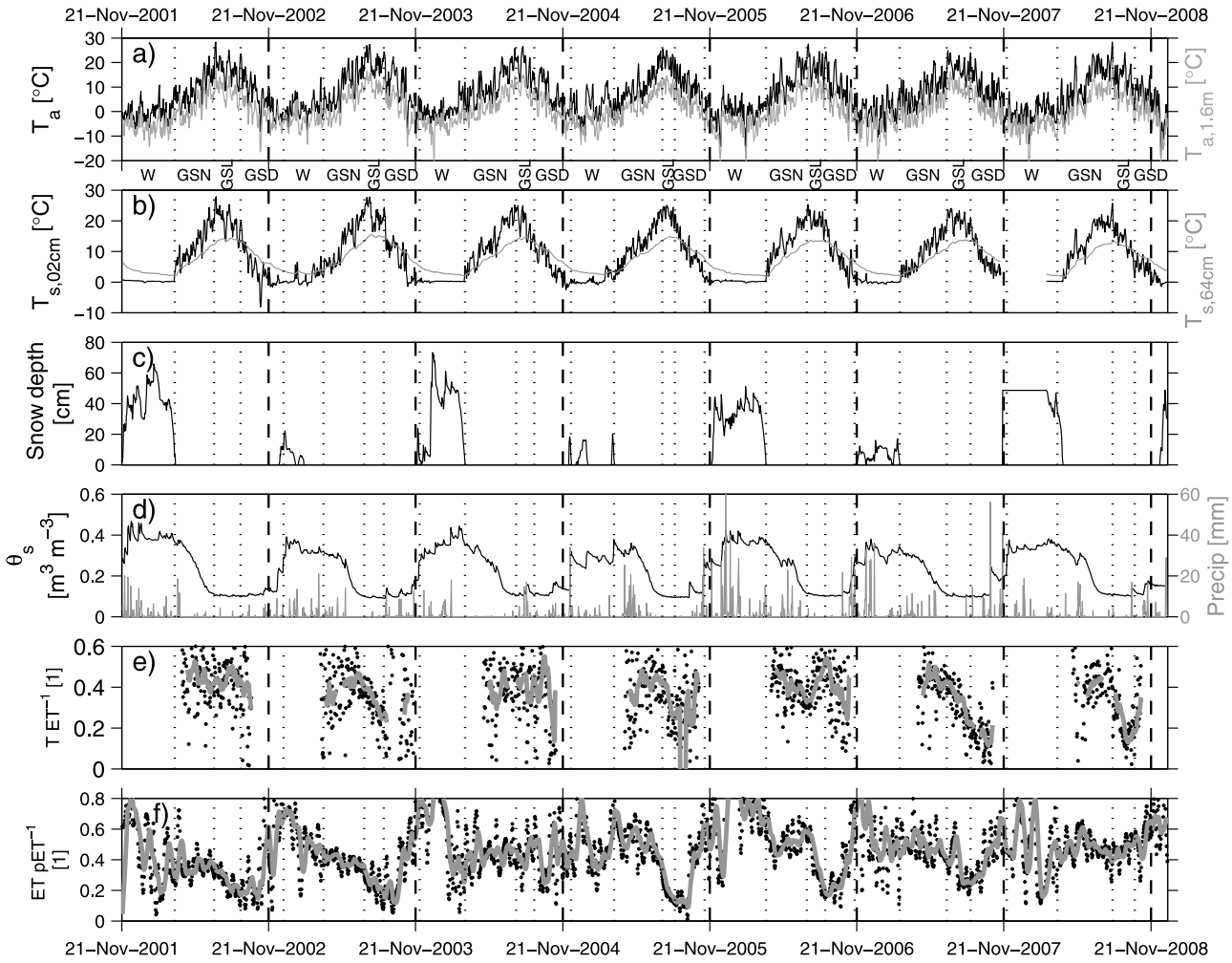

Figure 4. Daily aggregates of meteorological air and soil variables observed in the ponderosa pine forest in central Oregon: (a) above-canopy air temperature (T_a) and nighttime air temperature close to the ground ($T_{a,1.6m}$), (b) soil temperature at 0.02 and 0.64 m depth ($T_{s,02cm}$ and $T_{s,64cm}$), (c) snow depth, (d) surface soil water content integrated over the top 0.3 m (θ_s) and precipitation (precip), (e) ratio of tree transpiration to evapotranspiration (T ET^{-1}), and (f) drought index actual to potential evapotranspiration (ET PET^{-1}). Gray lines in Figures 4e and 4f are 2 week running averages. Vertical lines mark hydroecological years (bold dashed) and their seasons (light dotted) of winter (W), growing season nonlimited (GSN), growing season limited (GSL), and growing season drought (GSD). See section 3.3.1.

moisture starts to limit ET in a linear fashion. It is related to the vegetation wilting point θ_w and the soil field capacity θ_{fc} by the following inequality: $\theta_w < \theta^* < \theta_{fc}$ [*Hale and Orcutt*, 1987; *Nilsen and Orcutt*, 1996; *Waring and Running*, 2007]. θ^* at our site was determined through model optimization of a stochastic dynamic soil moisture model [*Miller et al.*, 2007]. When $\theta_s \geq \theta^*$, soil moisture does not exhibit control on stomatal activity of the plants.

[31] 2. The growing season nonlimited (GSN) represents the period of optimal growing conditions for plants as air temperatures and incident light are generally not limiting photosynthesis. Soil moisture is readily available to plants in liquid phase with $\theta_s \geq \theta^*$, but may become limiting toward the end when $\theta_s < \theta^*$ (Figure 4d). The onset of the growing season nonlimited is marked by the first day without snow cover or mean daily air temperatures $T_a \geq 0$°C during calendar year spring, whichever occurred later (Figures 4a and 4c). The vanished snow cover criterion was used in all but 1 (2003) year.

[32] 3. The physical significance of the growing season limited (GSL) is the increasing limitation of photosynthesis by increasing soil moisture stress, and it represents the transition period from the growing season nonlimited to the growing season drought. NEE in this season is reduced by limitations of GEP particularly in the afternoon hours (Figure 3b). The start of the growing season limited is given by $\theta_s \approx 0.1$ m^3 m^{-3} which is equal to the summertime minimum observed consistently across all years (Figure 4d).

[33] 4. The growing season drought (GSD) represents the period when both carbon and water fluxes are severely limited by soil moisture and plants are likely to experience drought stress. In growing season drought, θ_s and likely also the soil moisture in deeper layers are depleted. The onset is rather diffuse and was chosen according to maximum

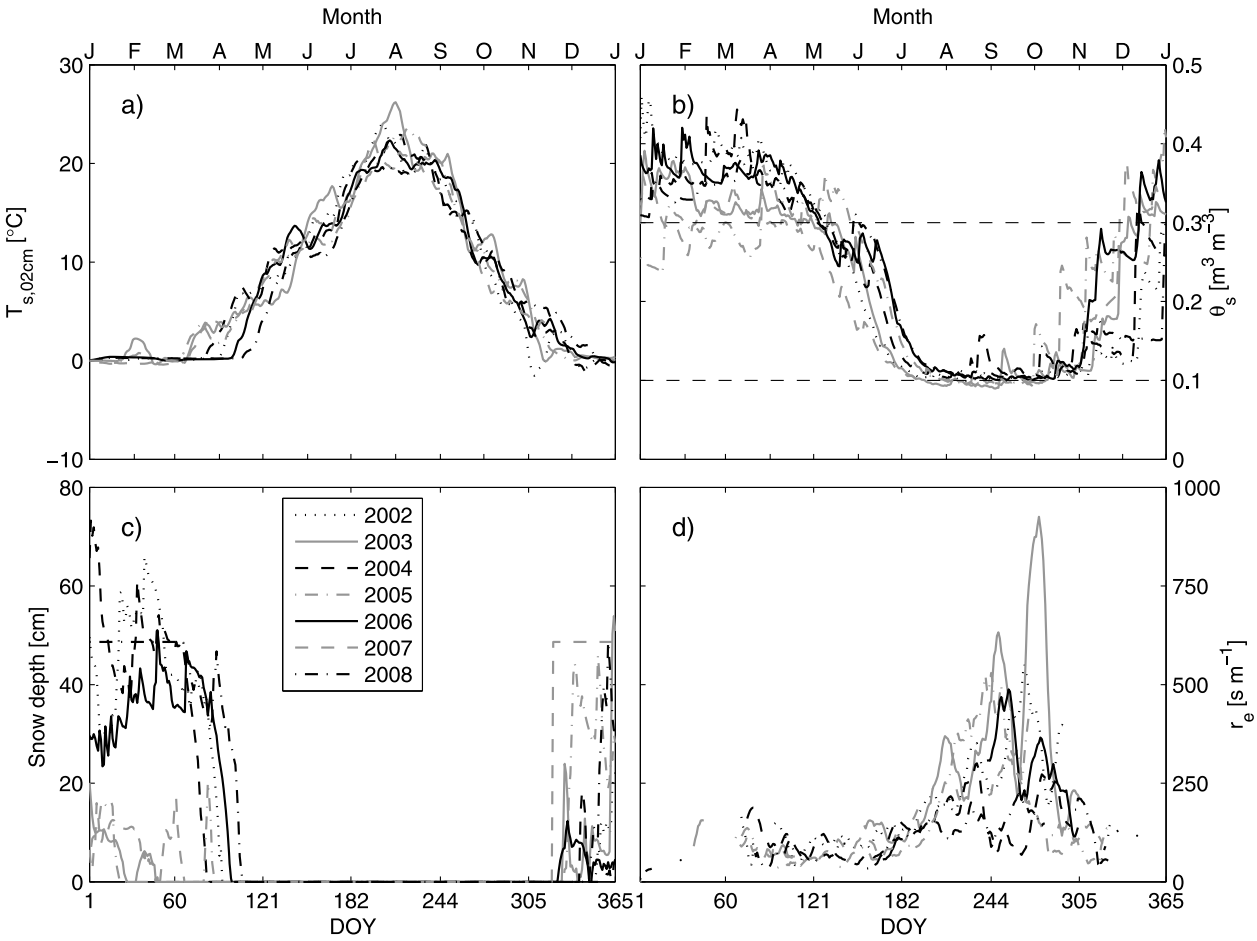

Figure 5. Interannual and seasonal variability of meteorological air, soil, and flux-derived variables used to delineate hydroecological years and their seasons as a function of day of calendar year (DOY): (a) surface soil temperature ($T_{s,02cm}$, 2 week running average), (b) surface soil water content integrated over the top 0.3 m (θ_s), (c) snow depth, and (d) maximum daytime ecosystem resistance (r_e, 2 week running average) derived from a Penman-Monteith model (see Appendix B). In Figure 5b, dashed lines mark thresholds to define seasonal transitions from growing season nonlimited to growing season limited (θ_s = 0.1) and from growing season drought to winter (θ_s = 0.3).

ecosystem resistance inferred by inverting the Penman-Monteith equation [*Penman*, 1948; *Monteith*, 1965] using measured latent heat flux time series (Figure 3f and Appendix B). An alternate start date can be found when the ratio of actual to potential evapotranspiration (ET/PET (Figure 4f)) exhibits its minimum. Both start dates closely coincided due to the physical connection between the parameters.

[34] We will hereafter refer to the hydroecological year and its seasons as defined above. An important a priori implication arising from the hydroecological year concept is that duration and timing of each season varies with site environmental conditions and therefore represents a direct measure of interannual and seasonal variability.

3.3.2. Seasonality Across Years

[35] Applying the concept of hydroecological years to the observations led to the seasonal and annual budgets for carbon and water fluxes listed in Tables 1 and 2. Lending to its definition, the start of the hydroecological winter was a reliable estimator for the onset of autumnal precipitation. We preferred observed θ_s over precipitation as the latter can occur in form of isolated events providing only insufficient moisture to alleviate plant water stress, which impedes the selection of a clear start date. In addition, soil moisture is a quantitative integral measure of all water inputs neglecting lateral groundwater movements. Although the soil moisture measurements are relatively shallow (0–30 cm), and these forests are known for hydraulic redistribution of deep soil water discussed later, the θ_s measurements capture the dynamic trends in seasonal water availability for ecosystem processes. The difference in start date of the hydroecological winter between the earliest (2006) and latest (2003) year was 51 days confirming the large interannual variability in water availability (Table 1 and Figure 5).

[36] Annual net carbon balance was dominated by seasonal uptake in growing season nonlimited contributing between 51% (2006) and 84% (2003) of the total. The analysis confirmed that this period is the primary season for carbon uptake with optimal environmental conditions, where the increase in GEP outweighed the increase in RE_{EC}. Similar values were observed in an evergreen oak forest in France were 83% of the net annual carbon sink

Table 1. Hydroecological Year Seasonal Statistics of Net Ecosystem Exchange, Gross Ecosystem Productivity, Ecosystem Respiration, and Actual Evapotranspiration From Eddy Covariance Data, Calculated Potential Evapotranspiration, Alternate Ecosystem Respiration Based on Soil Chambers on Foliage and Wood Respiration, and Tree Transpiration From Sap Flow Measurements and Ratios Thereof[a]

	Fractions					Ratios					
Season	NEE (%)	GEP (%)	RE_{EC} (%)	RE (%)	ET (%)	NEE/GEP[b]	|GEP/ET| (g C mm^{-1})	|GEP/T| (g C mm^{-1})	ET/PET[b]	Start DOY[b]	Duration (days)
HEY02[c]											
W	−4	13	18	18	19	−0.07	2.44	-	0.44	326 (2001)	130
GSN	78	45	34	37	46	0.42	3.52	9.88	0.33	91	98
GSL	14	29	33	31	24	0.12	4.24	10.09	0.23	190	65
GSD	11	14	14	15	11	0.19	4.55	-	0.18	255	70
HEY03[d]											
W	8	14	15	15	18	0.11	2.37	-	0.45	362 (2002)	99
GSN	88	47	37	39	48	0.37	2.93	7.26	0.36	96	102
GSL	−1	19	24	22	16	−0.01	3.68	11.39	0.19	198	48
GSD	5	20	23	24	18	0.06	3.24	-	0.33	245	116
HEY04											
W	8	14	17	14	14	0.15	3.4	-	0.49	335 (2003)	113
GSN	70	53	46	48	55	0.38	3.14	12.09	0.37	82	127
GSL	6	17	22	21	18	0.11	3.14	8.13	0.32	209	45
GSD	16	16	16	17	13	0.28	3.91	-	0.44	254	81
HEY05[c]											
W	22	20	19	18	17	0.34	4.28	-	0.42	345 (2004)	120
GSN	66	52	45	46	61	0.40	3.11	9.04	0.45	87	120
GSL	−1	10	15	14	8	−0.03	4.64	14.27	0.15	207	31
GSD	13	18	21	21	14	0.22	4.83	-	0.25	238	94
HEY06											
W	14	20	22	19	23	0.22	2.46	-	0.77	311 (2005)	145
GSN	52	41	36	43	50	0.40	2.34	6.42	0.46	99	101
GSL	14	18	20	21	18	0.24	2.96	7.45	0.32	201	46
GSD	19	20	21	17	10	0.30	5.57	-	0.23	246	73
HEY07											
W	3	9	12	15	13	0.11	2.37	-	0.55	319 (2006)	107
GSN	70	46	33	37	49	0.52	3.19	10.64	0.42	66	117
GSL	9	24	32	27	21	0.13	3.88	11.97	0.25	184	59
GSD	18	21	22	21	17	0.29	4.18		0.35	242	82
HEY08											
W	12	14	15	17	19	0.29	2.32	-	0.54	332 (2007)	126
GSN	68	57	52	54	57	0.40	3.09	11.2	0.42	93	137
GSL	14	20	23	19	16	0.24	3.71	16.99	0.42	230	55
GSD	6	9	10	10	8	0.23	3.31	-	-	285	48

[a]HEY, hydroecological year; NEE, net ecosystem exchange; GEP, gross ecosystem productivity; RE_{EC}, ecosystem respiration; ET, actual; PET, calculated potential evapotranspiration; RE, alternate ecosystem respiration; T, tree transpiration. Fractions are defined as seasonal divided by annual sums, and ratios are calculated between variables within a season. Also listed are the seasons' durations, which are sums. The hydroecological year starts 21 November, has 365 days, and is delineated into four functional seasons: winter (W), growing season nonlimited (GSN), growing season limited (GSL), and growing season drought (GSD). See sections 3.3 and 3.3.1 for details.

[b]Values are dimensionless.

[c]Years with moderate drought stress.

[d]Years with severe drought stress.

occurred between March and June [*Allard et al.*, 2008]. Conversely, Mediterranean-type grasslands showed their primary uptake season during the wet winter months outside of the conventional growing season [*Xu and Baldocchi*, 2004]. The ratio of growing season nonlimited to annual NEE was elevated in years experiencing severe drought stress (2002, 2003) as diagnosed by r_e, ET/PET, and anomalies in water year precipitation from the 26 year mean from 1982 to 2007 (Figure 7a). Despite the variability of NEE_{GSN}/NEE_{HEY}, the ratio of NEE_{GSN}/GEP_{GSN} showed little variability with a median of 0.40 ± 0.05 across all years with the exception of 2007, where the ratio was much larger. The reasons for this exception remained unknown. However, annual NEE/GEP showed variability across the observation period with severe drought years yielding smaller ratios (0.23) than other years (median 0.32 ± 0.05). Thus, variability in the annual ratio was caused by differences in seasons outside of the main net uptake period. The median annual ratio was slightly larger than that of 0.25 reported for an old growth ponderosa pine stand in close proximity [*Law et al.*, 2001b]. This may lend support to the hypothesis that the carbon sequestration efficiency of this mature stand was enhanced compared to the much older forest of similar species composition and environmental conditions.

[37] The constant seasonal NEE/GEP values in growing season nonlimited were consistent with the observation that calculated daily rates of GEP, RE_{EC} and NEE were similar across all years despite the large difference in start dates of 33 days for this season (Table 1). Note that a 1 month difference in onset leads to a large difference in available shortwave radiation. Thus, variability in springtime carbon dynamics was controlled by factors other than interannual variation in light conditions. The average daily rates for growing season nonlimited were -6.7 ± 0.6 and 3.9 ± 0.5 g C m^{-2} d^{-1} for GEP and RE_{EC}, respectively, resulting in a

Table 2. Comparison of Eddy Covariance Estimates of Net Ecosystem Exchange, Gross Ecosystem Productivity, Ecosystem Respiration, and Biological Estimates of Net Primary Productivity, Net Ecosystem Productivity, Autotrophic Respiration, and Alternate Ecosystem Respiration Based on Soil Chamber, Foliage, and Wood Respiration for Hydroecological and Calendar Years[a]

Hydroecological Year	NEE[b] (g C m^{-2} yr^{-1})	GEP[b] (g C m^{-2} yr^{-1})	RE_{EC}[b] (g C m^{-2} yr^{-1})	RE[b] (g C m^{-2} yr^{-1})	ET[b] (mm)	NEE/GEP[c]	|GEP/ET|[c] (g C mm^{-1})			
2002[d]	−376 ± 72	−1562 ± 203	1186 ± 202	976	434	0.24	3.60			
2003[e]	−251 ± 48	−1256 ± 163	1005 ± 171	1074	418	0.20	3.00			
2004	−503 ± 96	−1761 ± 229	1258 ± 214	1226	538	0.29	3.28			
2005[d]	−507 ± 96	−1613 ± 210	1106 ± 188	1110	440	0.31	3.67			
2006	−466 ± 89	−1484 ± 193	1018 ± 173	1057	530	0.31	2.80			
2007	−575 ± 109	−1690 ± 220	1115 ± 190	1032	497	0.34	3.40			
2008	−576 ± 110	−1718 ± 223	1141 ± 2194	1025	560	0.34	3.07			
Mean ± SD	−465 ± 116	−1583 ± 173	1118 ± 116	1071 ± 80	488 ± 57	0.29	3.26			
Calendar Year	NEE[b] (g C m^{-2} yr^{-1})	GEP[b] (g C m^{-2} yr^{-1})	RE_{EC}[b] (g C m^{-2} yr^{-1})	RE[b] (g C m^{-2} yr^{-1})	ET[b] (mm)	NEE/GEP[c]	|GEP/ET|[c] (g C mm^{-1})	NPP[b] (g C m^{-2} yr^{-1})	R_a[b] (g C m^{-2} yr^{-1})	NEP[b] (g C m^{-2} yr^{-1})
2002[d]	−386 ± 73	−1576 ± 205	1190 ± 202	974	441	0.24	3.57	408	656	90
2003[e]	−250 ± 48	−1253 ± 163	1003 ± 171	1082	415	0.20	3.02	443	724	85
2004	−538 ± 102	−1785 ± 232	1247 ± 212	1229	537	0.30	3.32	513	798	82
2005[d]	−472 ± 90	−1578 ± 205	1106 ± 188	1108	449	0.30	3.52	434	725	51
2006	−477 ± 91	−1503 ± 195	1026 ± 174	1052	530	0.32	2.84	493	707	149
2007	−572 ± 109	−1681 ± 219	1110 ± 189	1034	499	0.34	3.37	486	691	143
2008	−603 ± 114	−1741 ± 226	1138 ± 193	1023	561	0.35	3.10	484	692	201
Mean ± SD	−471 ± 121	−1588 ± 178	1117 ± 85	1072 ± 81	490 ± 56	0.29	3.25	466 ± 38	713 ± 44	114±52

[a]NEE, net ecosystem exchange; GEP, gross ecosystem productivity; RE_{EC}, ecosystem respiration; NPP, net primary productivity; NEP, net ecosystem productivity; R_a, autotrophic respiration; RE, ecosystem respiration. Net uptake of carbon is indicated by NEE < 0 and NPP; NEP > 0 due to different sign conventions. Uncertainty of annual NEE was estimated to ±19%, that of GEP was estimated to ±13%, and that of RE_{EC} and RE was estimated to ±17%; see text for details. SD is standard deviation.

[b]Values are sums.

[c]Values are ratios and are dimensionless.

[d]Years with moderate drought stress.

[e]Years with severe drought stress.

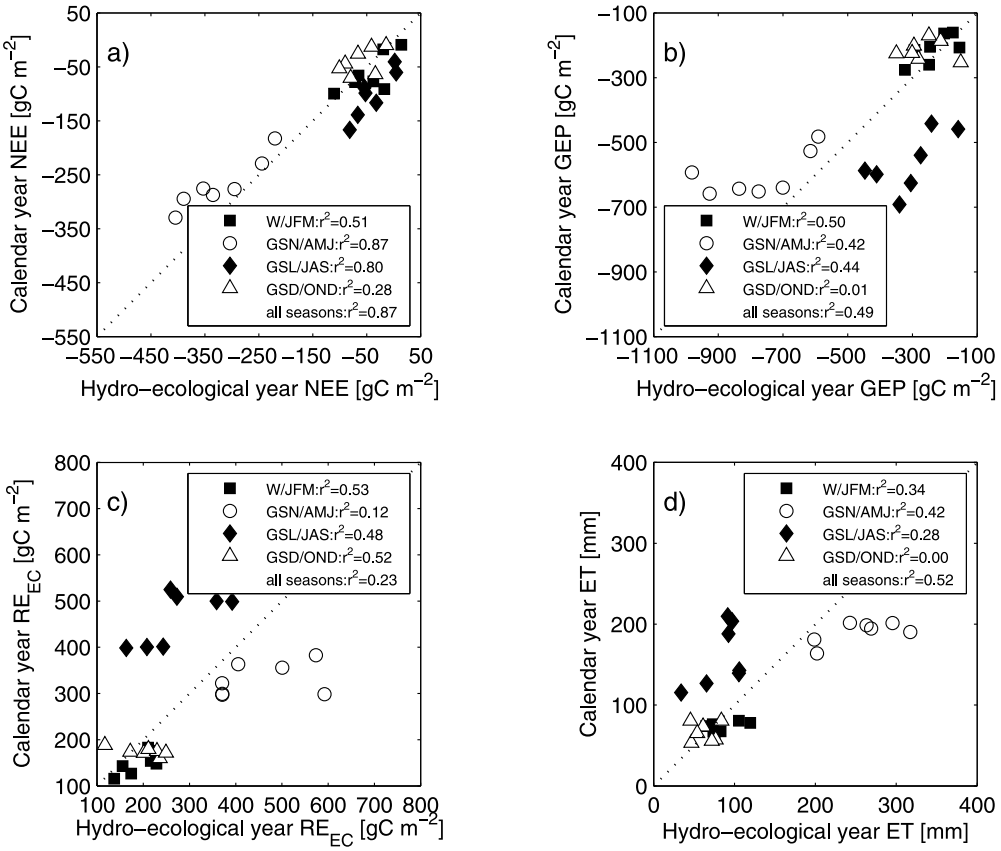

Figure 6. Comparison of hydroecological and calendar year seasonality in net ecosystem exchange (NEE), gross ecosystem productivity (GEP), ecosystem respiration (RE_{EC}) and evapotranspiration (ET) from eddy covariance measurements. Seasons of the hydroecological year are winter (W), growing season nonlimited (GSN), growing season limited (GSL), and growing season drought (GSD). Calendar year seasonality is winter (JFM), spring (AMJ), summer (JAS), and autumn (OND). Shown are coefficients of determination (r^2) for linear models.

net uptake of -2.8 ± 0.4 g C m^{-2} d^{-1}. In the subsequent growing season limited, photosynthetic rates were similar to the previous at -6.1 ± 0.8 g C m^{-2} d^{-1}, but respiration significantly increased to 5.5 ± 0.6 g C m^{-2} d^{-1} leading to a reduced net uptake of -0.6 ± 0.6 g C m^{-2} d^{-1}. The increase in respiration was attributed to rising soil and air temperatures and possibly to an additional signal from root growth associated with the peak in root production occurring in early summer [*Andersen et al.*, 2008]. Lending to the dominance in net carbon uptake during growing seasons nonlimited and limited, we will hereafter refer to them collectively as the "active period" further discussed in section 3.3.4.

[38] Identification of seasonal key environmental drivers improves process knowledge and facilitates modeling of ecosystem fluxes. Therefore, stepwise correlation analysis was employed to identify environmental controls on seasonal carbon and water exchange in growing seasons nonlimited and limited. Out of the tested environmental variables (T_a, R_g, θ_s, and seasons' duration), only cumulative θ_s and duration yielded significant correlations with seasonal GEP and RE_{EC}, whereas mean θ_s, T_a and R_g failed to yield any significant relationships. Cumulative quantities should be preferred over averaged quantities whenever the integral of a variable is more meaningful to ecosystem processes and functioning than its mean. As an example, the reservoir of soil moisture essential for photosynthesis is better captured by its temporal integral (sum) than its mean (sum/duration). However, photosynthetic rates are better explained by mean light conditions which gives rise to the use of light response curves in modeling exercises. Temperature threshold behavior of trees can be either sensitive to integrals (e.g., temperature sums to explain bud break), or mean and incident values (e.g., temperature dependency of root respiration). Vapor pressure deficit (VPD) was not selected for this analysis, as it is strongly cross correlated to global radiation, air temperature, and possibly θ_s. Note that VPD, T_a, R_g are known to exert a strong control on subweekly and monthly time scales through their link to stomatal conductance [*Law and Waring*, 1994]. However, these shorter than seasonal time scales are outside the scope of this paper. GEP was found to become more negative (more carbon gain) and RE_{EC} to increase (more carbon loss) with increasing available θ_s in a linear fashion ($r^2 \geq 0.75$). Cumulative θ_s was statistically correlated to duration of all seasons ($r^2 \geq 0.80$), which was not surprising since the hydroecological seasons were primarily defined based on the site hydrology. Air temperatures in growing season nonlimited explained variation (residuals) in GEP and RE_{EC} after removing the dependency on θ_s, indicating more net

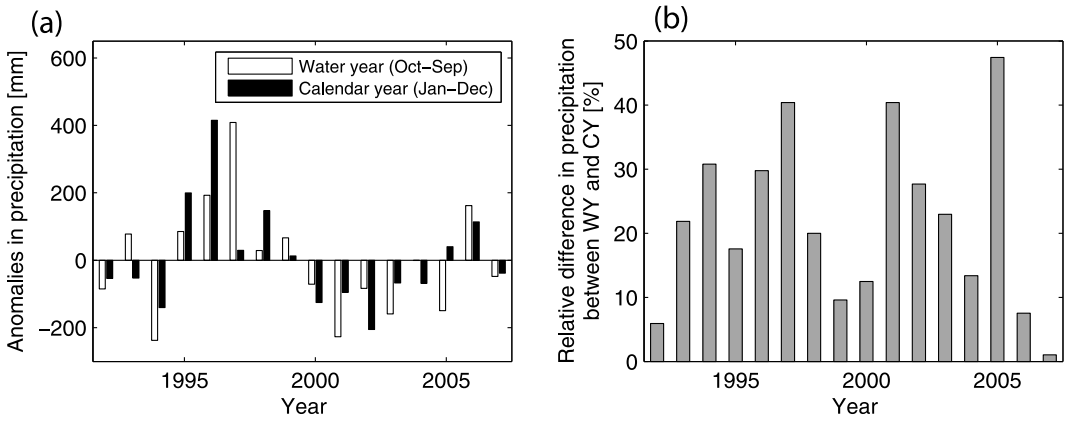

Figure 7. (a) Annual precipitation anomalies from the 26 year climatologic mean (1982–2007) calculated for water years (WY, October–September) and calendar years (CY, January–December). (b) Also shown are relative differences in precipitation between the two aggregation schemes. The use of calendar year precipitation would lead to a false interpretation of 2002 as the driest year, which emphasizes the importance of using water years or hydroecological years to diagnose droughts. Precipitation data are monthly spatially interpolated data of 800 m resolution at the study site (source is PRISM Group, Oregon State University, http://www.prismclimate.org).

carbon uptake with rising temperatures. One may argue that the concept of hydroecological years biases seasonal and interannual variability of carbon and water exchange toward a strong correlation with hydraulic variables. However, one must note that (1) only the onsets of the hydroecological winter and growing season limited were selected directly based on θ_s leaving all other transitions depending on air temperature, snow cover or ecosystem resistance, which might have an indirect dependency on θ_s only, and (2) the gap-filling models used calendar year divisions not coinciding with hydroecological seasons (see Appendix A). In summary, seasonal carbon dynamics were primarily dependent on the amount of plant-available soil moisture, whereas air temperatures exerted a secondary, but much weaker control.

3.3.3. Comparing Hydroecological to Calendar Year Seasonality

[39] Calendar year delineation was applied to highlight the improvements of hydroecological seasonality on the interpretation of environmental controls of carbon and water exchange. The simplest division of seasons within a calendar year follows the climatologic conventions of winter (JFM), spring (AMJ), summer (JAS), and autumn (OND). These seasons and other multimonthly aggregates are often used in cross-site comparisons and large-scale modeling exercises covering different biomes as they provide a convenient means to compare seasonal responses over a large number of sites. We acknowledge that many carbon cycle studies use a more sophisticated scheme for seasonal differentiation than the basic 3 month divisions, yet we believe that the comparison is valuable as implications for drought limited ecosystem were profound.

[40] Despite the negligible differences in annual gross and net carbon fluxes and ET (Table 2), large differences were observed in seasonal fluxes (Figure 6). The agreement among annual budgets was not surprising given the fact that the general annual course of carbon and water fluxes can be described by a semiperiodic wave pattern. Based on this approximation, hydroecological and calendar year budgets represent integrals over the same period at a small phase shift.

[41] None of the tested environmental variables (T_a, R_g, θ_s) yielded significant correlations with NEE, GEP or RE_{EC} in any calendar year season. A direct comparison of budgets between equivalent seasons produced a reasonable agreement for net carbon fluxes, but also demonstrated the poor coherence for GEP, RE_{EC} and ET (Figure 6). In particular, correlation of ecosystem respiration was poorest ($r^2 = 0.23$). Calendar year component fluxes of GEP, RE_{EC}, and ET peaked later in the year compared with their hydroecological equivalents, leading to the interpretation of the summer months (JAS) being the most physiologically significant period. This interpretation is counterintuitive given both the soil water limitations (Figures 3d and 4d) and the resulting observed limitations to soil respiration and photosynthesis (Table 1) [*Law et al.*, 1999; *Irvine et al.*, 2008].

[42] We also compared the usefulness of patterns in precipitation anomalies between calendar year and the conventional water year delineation for the purpose of identifying droughts (Figure 7). Calendar year anomalies poorly captured the large variability in winter precipitation and the associated onset of the hydroecological winter, whereas water year divisions were more adequate. In the two decades bracketing the observation period, the 3 driest years were observed in 2002, 2000, and 2003 according to calendar years, whereas aggregation by water years returned 2001, 1994, and 2003. The 26 year average annual precipitation over the period 1982–2007 (PRISM data) was 535 ± 41 mm for calendar, and 540 ± 43 mm for water year analysis. Two of the top three years with the largest differences between the aggregation schemes fell into the observation period (2001: 40%, and 2005: 47%). From a hydrological and plant ecological perspective, precipitation occurring at the end of a calendar year must be counted toward the next vegetation period as it replenishes soil water available for plant growth the following calendar year. The discrepancy in identified drought years will be important for the discussion of carbon and water coupling below.

3.3.4. Growing Season Length

[43] The consistent and large photosynthetic rates observed in growing seasons nonlimited and growing season limited provided one possible definition of an active period in this forest. Spring air temperatures coinciding with snowfall and the summer soil water depletion therefore delineated the active period, and its length spanned the duration of its two contributing seasons. The terminology was intentionally chosen to be different from "growing season length" to emphasize their conceptual differences. A common definition of a growing season length is given by the number of days exceeding a species-specific temperature threshold or cumulative temperature sums [cf. *Waring and Running*, 2007]. We hypothesize that if the active period captures physiological activity in ponderosa pine, one would expect photosynthesis and possibly net carbon uptake to correlate with environmental variables controlling plant physiology during this period, but not necessarily ecosystem respiration assuming that a major fraction is contributed by heterotrophic respiration subject to different controls.

[44] Active period GEP and ET were statistically significantly correlated with cumulative θ_s (not shown here), whereas no clear relationship between RE_{EC} and T_a, R_g, θ_s could be found, which corroborated the above hypothesis. Our results were coherent with those found in a Mediterranean grassland where timing of precipitation and available soil moisture had a larger impact than total annual precipitation on ecosystem GPP and NEE [*Xu and Baldocchi*, 2004] despite the differences in timing of the peak growing season described earlier. Phenological observations at an old growth ponderosa pine forest in close proximity to the study site showed that the completion of needle elongation coincided with the transition from growing season limited to growing season drought, which underlined the ecological significance of the active period. The hydroecological seasonality collapsed years with severe, moderate and very little drought stress on to a common, linear dependency on plant-available soil water, whereas any seasonality based on air or soil temperatures would fail as variability in θ_s outweighed those in T_a and T_s (Figure 5). The length of the active period varied by 45 days. The variability of the end date (47 days) exceeded that of the start date (33 days). This finding was contrary to our initial hypothesis, but can be explained by the larger variability in summer soil moisture compared to that in springtime air temperatures and snowmelt. Overall, active periods in years with severe drought stress were shorter than in moist years.

[45] Active period NEE was linearly related to its duration (Figure 8a). This relationship may prove useful to predict net carbon uptake in future climates: Active period NEE, which comprises the majority of annual net carbon uptake, could be approximated by simply analyzing air temperature and surface soil moisture observations delineating the active period. An active period of 190 days explained the 7 year annual mean NEE of -465 ± 121 g C m^{-2} (see Table 2). *Ma et al.* [2007] also found that interannual variability in NEE was mainly related to growing season length in a Mediterranean-type savanna, a grassland, and an evergreen oak ecosystem in Northern California. Ecosystem and tree water use efficiencies linearly increased with increasing water stress during the active period (Figure 8b) with no obvious differences between dry and moist years suggesting that ponderosa pine can adapt well to increasing water stress.

3.4. Carbon-Water Coupling

[46] Evidence for carbon-water coupling was also provided by the following observations in addition to those already discussed for the active period: First, the depletion of surface soil moisture to its summertime minimum coincided with a decrease in daily net carbon uptake within a few days. The reduced uptake rate led to a visible breakpoint in the cumulative NEE time series. Note that the coincidence of the two events was not an artifact of the hydroecological year concept, but can be interpreted as physiological response of the trees to the increasing soil moisture stress linked to rooting depth. In 2001 (DOY 307), profile sampling of live fine root carbon mass to 1 m depth at 15 locations indicated that 34% of the mass was located in the top 0.2 m depth, and 29% in the 0.2–0.5 m depth resulting in a total of 63% concentrated in the top 0.5 m (126 of 200 g C m^{-2}). In addition to the obvious connection between NEE and θ_s due to the shallow rooting depth, soil moisture in deeper layers may still be important. Assimilation rates were almost unchanged throughout the active period despite the fact that θ_s was already depleted in growing season limited, which composed the later part of the active period (Figure 4d). The loss of θ_s alone explained seasonal ecosystem ET in the first part of the active period during growing season nonlimited, but not later (Figure 8c). Tree transpiration (T) from sap flow measurements was approximately 50% of total ET, which was in agreement with mean daily T ET^{-1} ratios (Figure 4e). Intraseasonal dynamics of T, ET, and the depletion of θ_s showed a large variability with a general trend toward larger evapotranspirative loss early in the active period followed by a decline. These results in connection with the linear correlation of growing season nonlimited GEP to cumulative θ_s (not shown here) pointed also to a strong coupling between carbon uptake and surface soil moisture. However, deeper water must also be accessible to trees and other smaller plants in the summer months, as the depleted θ_s and the decreased ratio T ET^{-1} could not explain the ET loss (Figures 8c and 4d–4f). A study in an old growth ponderosa pine forest in close proximity showed a steady decline in soil water storage below 0.6 m depth as summer drought progressed, and hydraulic redistribution of deep soil water to the upper soil layers led to some compensation of surface soil moisture deficit where the density of fine roots was the greatest [*Brooks et al.*, 2002]. Continuous observations of time- and depth-dependent dynamics of soil moisture down to 1.6 m depth (Sentek EnviroSmart probes, Sentek Sensor Technologies, Stepney, South Australia, Australia) commenced only in 2006, so a full record over the 7 year period was not available. Interannual variability in θ_s and snow cover showed a qualitative relationship with deeper snowpack and higher snow water equivalents being positively correlated to higher θ_s (Figures 5c and 5d), which may serve as a proxy for hydrologic recharge in greater depths.

[47] Second, GEP and ET were significantly correlated ($r^2 \geq 0.67$) in the active period, resulting in a mean ecosystem water use efficiency (WUE = GEP ET^{-1}) of

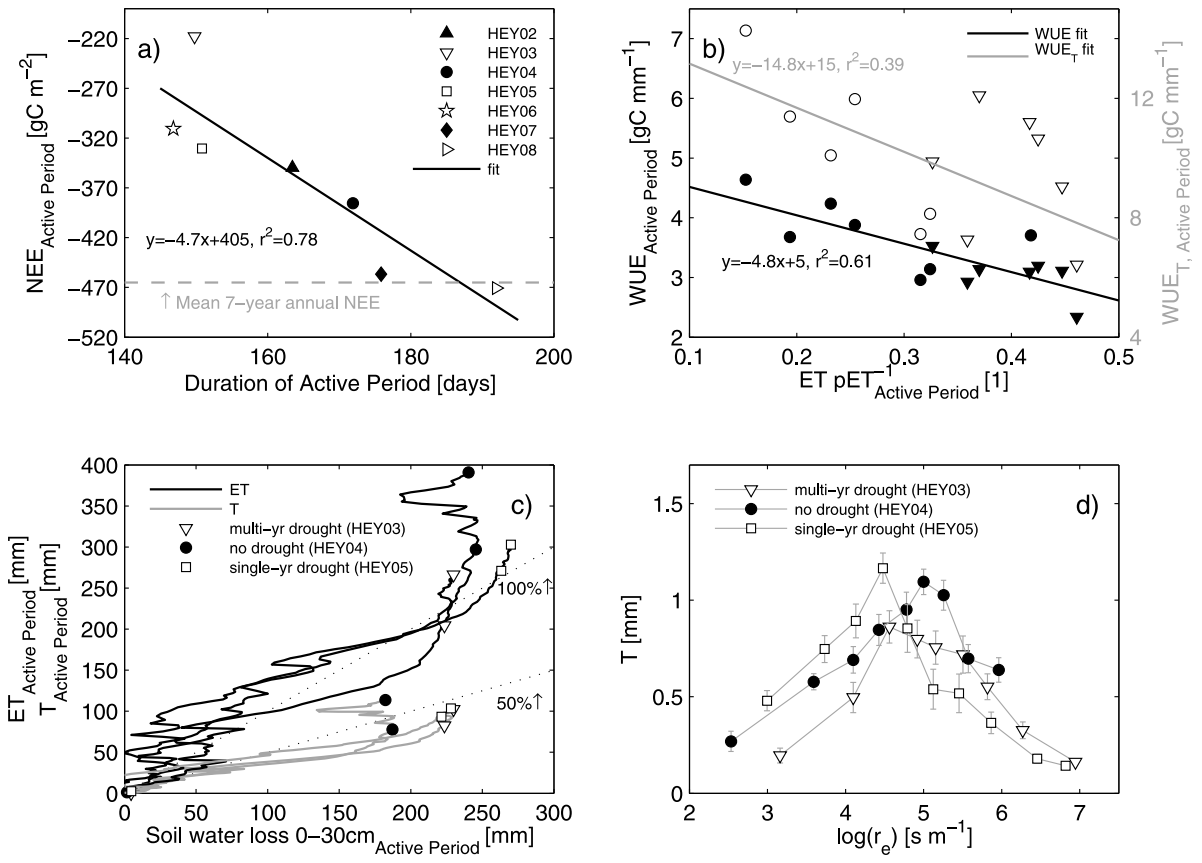

Figure 8. Carbon and water exchange during the active period (growing season nonlimited and growing season limited): (a) net ecosystem exchange ($NEE_{Active\ period}$) versus duration, (b) ecosystem water use efficiency (WUE, solid) and tree water use efficiency (WUE_T, open) versus drought index actual to potential evapotranspiration (ET PET^{-1}), (c) actual evapotranspiration (ET) and tree transpiration (T) versus surface soil moisture loss, and (d) tree transpiration as a function of ecosystem resistance (r_e) for a multiyear drought, no drought, and a single-year drought. Symbols in Figure 8b are growing season nonlimited (circle) and growing season limited (triangle). Markers in Figure 8c depict start and end dates of hydroecological seasons (see section 3.2.1). Equations are shown for linear models with coefficient of determination (r^2). Bars are standard errors.

2.7 and 3.4 g C mm^{-1}, respectively (see also Table 1). The tree water use efficiency (WUE_T = GEP T^{-1}) showed the same seasonal increase, but ratios were larger by a factor of 3, amounting to 9.9 and 11.4 g C mm^{-1}, respectively. The tight coupling of GEP and ET pointed to carbon-water coupling through stomatal control particularly when surface soil moisture was depleted resulting in a VPD increase during the later part of the active period. The interannual variability in T ET^{-1} was larger in growing season nonlimited compared to growing season limited. Stomatally controlled transpiration was therefore the dominant component of ET during significant dry periods when soil evaporation is minimal. In general, T ET^{-1} ratios declined with increasing drought stress, suggesting that the fraction of tree transpiration decreased with decreasing θ_s (Figure 4e). θ_s minima in growing season limited were higher in years with deeper and prolonged winter snow cover (hydroecological winters in 2002, 2004, 2006) than in years with little snowpack. The severity of the summer drought may therefore be closely associated with the hydraulic recharge of deeper soil layers from snowmelt. Declining ratios T ET^{-1} with decreasing θ_s were counterintuitive as one would expect the contribution of tree transpiration to increase because of the access to deeper soil moisture and the sharp decline of evaporation caused by the exhausted shallow soil water. However, *Irvine et al.* [2004] made the same observation and concluded that the nontree, i.e., shrub transpiration, is a major component in late summer ET not captured by the sap flow measurements. Evaporation of canopy interception is unlikely to play a significant role during the drought due to the lack of rain and dewfall. Moreover, it should be noted that, even though θ_s is low during summer, bare soil evaporation might still significantly contribute to ET given high air temperatures and thus high evaporative demand and force vertical recharge from deeper soil moisture profiles.

3.5. Drought Response

[48] The interannual variability of precipitation provided the opportunity to evaluate the ecosystem response to drought stress on various time scales. A series of anomalous dry years occurred during 2001–2003 with annual water year precipitation being 42%, 15% and 29%, respectively,

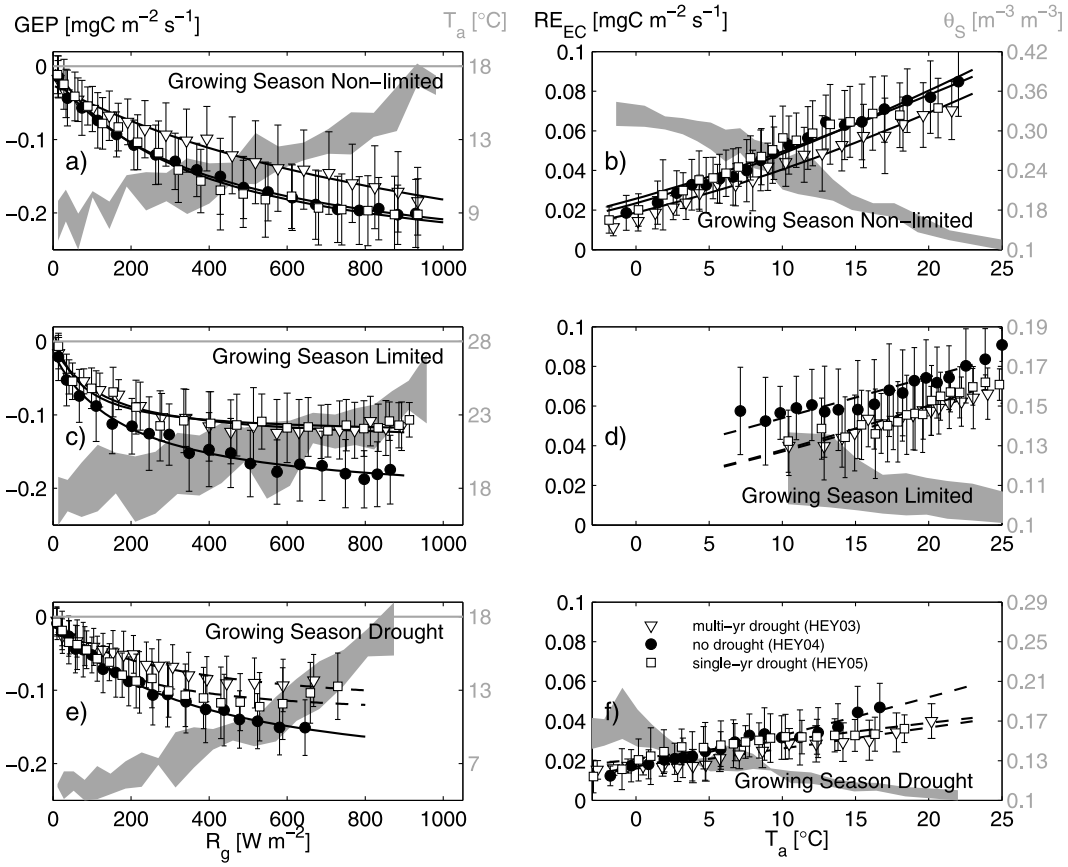

Figure 9. (a, c, e) Light response curves of gross ecosystem productivity (GEP) as a function of incident shortwave solar radiation (R_g) for different hydroecological seasons. Gray shaded areas depict variability of air temperature (T_a) in the radiation bins. (b, d, f) Temperature response functions of ecosystem respiration (RE_{EC}) for the same hydroecological seasons, with gray areas reflecting variability in surface soil water content (θ_s). Error bars are standard deviations within each bin.

lower than the 26 year average of 540 mm (data from PRISM Group, Oregon State University, http://www.prismclimate.org). After alleviation of the drought in 2004, precipitation in the subsequent year of 2005 was lower by 28%, but the drought did not extend more than 1 year. We therefore selected the sequence of hydroecological years 2003–2005 to evaluate the differences in ecosystem response to multiyear versus single-year droughts with 2004 being the control case representing no severe seasonal water limitations. The seasonal development of GEP as a function of R_g (light response curves) showed that GEP rates at the end of the multiyear drought were reduced compared to the no-drought case in all growing seasons (Figures 9a, 9c, and 9e). Conversely, GEP in growing season nonlimited of the single-year drought was not different from the control case, but effects of the water limitations on GEP started to occur only in the subsequent growing season limited. Differences in photosynthetic rates for a given light intensity could not be explained by temperature sensitivity of photosynthesis, although the variability of T_a in the 3 year sequence was maximized in summer. At moderate light intensities ($R_g \approx 600$ W m^{-2}), the reduction of GEP equaled 20%, 40% and 40% in growing season nonlimited, limited, and drought, respectively, in case of the multiyear drought, and 0%, 40%, and 25% in case of the single-year drought. The decline of growing season drought GEP with increasing light intensities beyond 600 W m^{-2} in dry years was caused by an increasing VPD discussed above. The drought response in RE_{EC} was similar in growing season limited and growing season drought yielding no differences between the multiyear and single-year droughts (Figures 9b, 9d, and 9f). The net effect of the multiyear drought resulted in the lowest annual NEE for hydroecological year 2003 (44% lower than the 7 year average), because the reduction in GEP was proportionally larger than that in RE_{EC} (23% versus 15%). In case of the single-year drought, the net effect was negligible resulting in 9% increase compared to the 7 year average and a slightly larger response in RE_{EC} compared to that in GEP. Annual litter fall also peaked at the end of the multiyear drought suggesting that the trees were not able to support and maintain a canopy similar to that of years without above average water limitations (Figure 2). This response was likely caused by carryover effects of reduced carbohydrate reserves in plant tissue in combination with poor soil moisture recharge in greater depths. The extreme litter fall may have caused RE_{EC} to peak the following year due to the associated increase of heterotrophic respiration from fast turnover litter pools. Soil CO_2 efflux, which includes the influence of litter decomposition, was highest in 2004 [*Irvine et al.*, 2008]. Decomposition of additional litter may therefore represent another carryover effect impacting

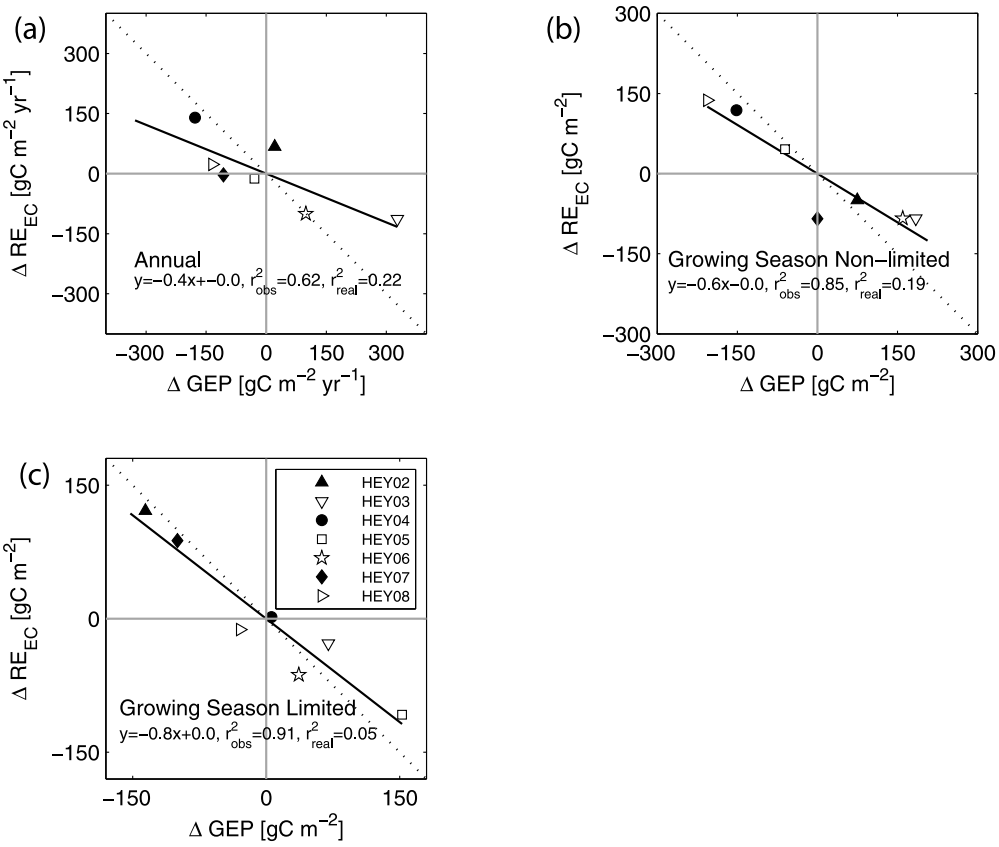

Figure 10. Comparison of annual anomalies in gross ecosystem productivity (GEP) and ecosystem respiration (RE_{EC}) from the 7 year hydroecological means: (a) annual, (b) growing season nonlimited, and (c) growing season limited. Equations are shown for linear models with observed coefficient of determination (r^2_{obs}) and the resultant real coefficient of determination (r^2_{real}) after correcting for spurious self-correlation.

the postdrought carbon balance with proximate component-specific effects and indirect effects on NEE.

[49] Tree transpiration could also serve as an indicator of drought severity as it is linked to deeper soil water by rooting depth. For a given ecosystem resistance, tree transpiration showed a clear response to duration of the drought (Figure 8d). It was lower at the end of the multiyear drought compared to the single-year or the control case, and in both cases, T peaked at lower ecosystem resistances.

3.6. Coupling Between Photosynthesis and Respiration

[50] Annual anomalies in photosynthesis and respiration suggested that interannual variability in NEE was dominated by changes in GEP rather than RE_{EC} with a regression slope of −0.4 (Figure 10). However, one has to exercise great caution when interpreting such plots for ecosystem behavior as the real coefficient of determination is only $r^2 = 0.22$ after accounting for the artificial self-correlation arising from the flux partitioning algorithm [*Vickers et al.*, 2009b]. NEE in both seasons of the active period confirmed this results, but yielded even smaller real r^2 because of the increased variability in RE_{EC} (i.e., the shared variable) compared to that of NEE, which is in agreement with the analytical framework of the spurious self-correlation problem [*Kenney*, 1982]. We acknowledge that a true physiological connection between RE and GEP is likely to exist, but emphasize that its evaluation and quantification is difficult given the limitations arising from the flux partitioning method deployed here.

[51] The ratio of autotrophic respiration to photosynthesis ($|R_a/GEP|$) was found to be conservative on annual time scales with a median of 0.45 ± 0.06 with the exception of 2003. We recall that 2003 was the last year of a multiyear drought showing severe water limitations and a culmination of carryover effects. In that year, $|R_a/GEP|$ was larger (=0.58) pointing to an increased autotrophic respiration possibly caused by the increased use of carbohydrate reserves in the plant tissue. Reserves were exhausted at the end of the active period the same year likely causing the extreme litter fall. The increased R_a in 2003 could not be explained by the slightly higher mean summer temperatures (18.0°C) compared to all other years (16.7°C) resulting in an increase of approximately 10%, 11%, and 5% in foliage, wood and soil chamber respiration, respectively.

3.7. Regional and Interdecadal Context

[52] Anomalies of annual precipitation and mean air temperature for the site were compared to those recorded at several observational stations in close proximity with a longer record in an effort to place the results of the 7 year observation period into a regional and interdecadal context (Figures 11a and 11b). Three sites of the SNOTEL monitoring network for water and climate operated by the

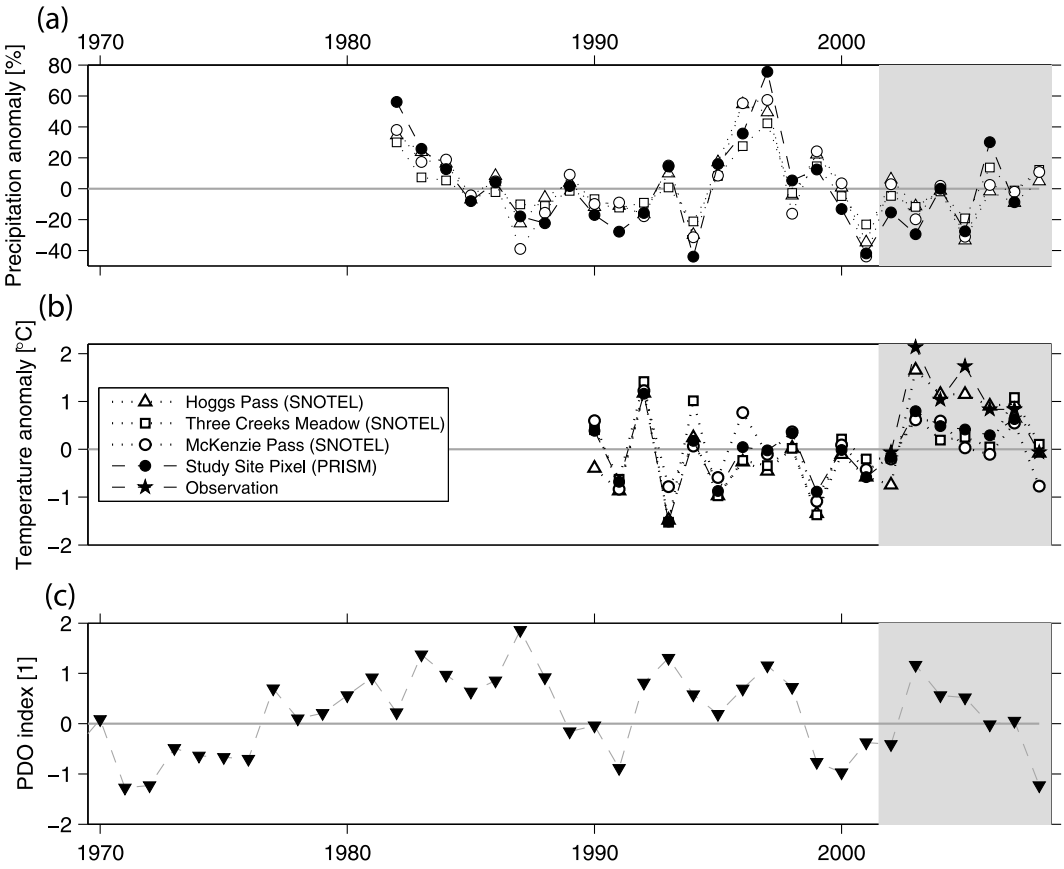

Figure 11. Interdecadal and regional context of the 7 year observation period (2002–2008, gray area). (a and b) Precipitation and air temperature anomalies in reference to their 18 year climatologic mean in water years (1990–2008) at three SNOTEL sites (Hoggs Pass, 44.42°N, 121.85°W, 1450 m above sea level; Three Creeks Meadow, 44.15°N, 121.63°W, 1722 m; McKenzie Pass, 44.20°N, 121.87°W, 1463 m) operated by the Natural Resources Conservation Service of the U.S. Department of Agriculture in close proximity to the study site, for the PRISM site pixel (data from PRISM Group, Oregon State University, http://www.prismclimate.org) and site observations. (c) Pacific Decadal Oscillation (PDO) index.

Natural Resources Conservation Service of the USDA provided continuous observations of mean air temperature between 1989 and 2007, and precipitation between 1982 and 2007. The 7 year site record was extended using available PRISM precipitation data, and mean air temperature was calculated from PRISM minimum and maximum monthly temperatures using an empiric formula for the same period [*Thornton et al.*, 1997]. Anomalies in both precipitation and air temperature were in phase and interannual patterns agreed well across all sites. The 7 year observation period was drier and warmer in reference to the 20 year record preceding 2007. The 1990s were characterized by a generally higher than average precipitation particularly in the second half between 1995 and 1997, whereas clear trends in temperatures were absent. Starting in 2000, precipitation declined below average reaching its minimum in 2001. Trends in temperature were slightly offset and indicated warmer conditions starting 2003. The Pacific Decadal Oscillation (PDO [*Mantua et al.*, 1997; *Zhang et al.*, 1997]) index was primarily positive in the observation period suggesting a warm PDO regime (Figure 11c). The PDO is a long-lived El Niño–like pattern of Pacific climate variability with a typical event length of 20–30 years in the past century. Its climatic fingerprints are most distinct in the North Pacific/North American sector rather than the tropics. The PDO index is defined as the leading monthly sea surface temperature anomaly in the North Pacific Ocean pole ward of 20°N. For western North America, the general PDO-related temperature and precipitation pattern in warm phases (positive index) are above average winter and spring temperatures associated with below average precipitation. For cool phases (negative index), these patterns are reversed. The observed air temperature and precipitation anomalies were coherent with the definition of PDO phases. The inherent variability of the PDO index and the current poor physical understanding of the underlying atmospheric and oceanic circulations and feedback mechanisms do not allow for predicting mean future precipitation and temperature conditions at the site.

4. Conclusions and Implications

[53] We arrived at the following conclusions with regard to our leading hypotheses based on 7 continuous years of micrometeorological and biological measurements of car-

bon and water exchange in a semiarid ponderosa pine ecosystem.

[54] 1. Interannual and seasonal variations of carbon and water exchange were best explained when seasonality was defined functionally within a hydroecological year. In comparison, an analysis employing calendar year–based seasonality suggested a shift of the main net carbon uptake, and active fluxes of photosynthesis, ecosystem respiration, and evapotranspiration toward later seasons when soil moisture availability was already limited. The concept of hydroecological years was therefore essential to reveal dynamics of carbon and water exchange in this summer drought-stressed ecosystem, which would have gone undetected otherwise. Application of the hydroecological at other sites will require a redefinition of thresholds and key events depending on the site hydrology.

[55] 2. Growing season length, here redefined in terms of the active period with maximized photosynthesis within a hydroecological year, was the dominant factor in annual carbon and water cycle dynamics, and found to be linearly related to plant-available soil moisture. The net carbon sequestration occurring during the active period accounted for between 65% and 96% of annual NEE, and 66% and 73% of evapotranspiration in a given year. Contrary to our hypothesis, the variability of the end date exceeded that of the onset due to the larger variability in soil moisture during the summer months. No evidence was found that would support a correlation between the active period start date and annual net carbon uptake. Photosynthesis and ecosystem respiration did not yield significant correlations with global radiation and air temperature on seasonal and annual time scales.

[56] 3. The interannual variability of NEE of carbon dioxide is driven by variability in GEP, which is determined by plant-available soil water during the active period. Plant-available soil water is therefore the main determinant of net carbon uptake in this ecosystem, in support of *Granier et al.*'s [2007] finding of significant soil water control on carbon and water dynamics at 12 European monitoring sites during the 2003 drought. Spring air temperatures and thus vapor pressure deficits during the main uptake period were a secondary determinant only.

[57] 4. Seasonal carbon and water fluxes were tightly coupled through soil hydrology and stomatal activity. Ecosystem and tree water use efficiencies were conservative across the years, and exhibited similar seasonal patterns showing increasing efficiency with increasing water limitation. The contribution of soil evaporation and nontree species to ecosystem evapotranspiration becomes particularly important in anomalously dry years, when tree water and carbon exchange is severely limited.

[58] 5. The ponderosa pine ecosystem responded differently to multiyear compared to single-year drought stress in a nonlinear fashion. Net carbon uptake was found to be significantly reduced at the end of a 3 year drought period, but showed no response to a single dry year. This finding emphasizes the need to explicitly account for carryover effects in both observations and models when investigating interannual dynamics and coupling of ecosystem-scale carbon and water exchange.

[59] 6. Analysis of regional temperature and precipitation patterns over the period 1982–2007 placed the 7 year observation into the context of a warm cycle of the Pacific Decadal Oscillation (PDO) characterized by above average temperatures and below average precipitation. It is therefore conceivable that net carbon uptake would increase during a cool PDO cycle typically associated with opposite precipitation and temperature trends assuming that the ecosystem is able to store the additional water for plant growth during the active period.

Appendix A: Eddy Covariance Data Processing

[60] We chose a fixed perturbation and averaging time scale of 30 min for nighttime and daytime data as a good compromise between systematic and random errors inherently associated with this type of flux calculation scheme. This selection was based on an investigation of measurement uncertainty for CO_2 fluxes at the study site demonstrating that 30 min averages were acceptable for longer-term aggregates of net ecosystem carbon and water exchange [*Vickers et al.*, 2009a].

[61] Postprocessing of raw data recorded on memory cards was done off-site for all years except 2002 when covariances and high-order statistics were calculated online and stored in the loggers' memory. Outliers from raw time series of turbulent variables were removed using a despiking routine [*Vickers and Mahrt*, 1997] and plausibility limits (Figure A1). Carbon dioxide and latent heat fluxes were corrected for density fluctuations using the post hoc method [*Webb et al.*, 1980]. Raw EC 30 min flux estimates were subject to rigorous quality control using a combination of higher-order statistics and quality flags for stationarity [*Foken and Wichura*, 1996] and developed turbulence [*Thomas and Foken*, 2002] following the methodology described by *Foken et al.* [2004]. As a result, a large fraction of nocturnal CO_2 fluxes (F_c) were rejected because of the strong prevailing temperature inversions accompanied by weak winds leading to suppressed turbulent exchange. In addition, nocturnal EC flux data were excluded for Northerly flows as estimates were systematically lower compared to alternate ecosystem respiration using the chamber approach. Raw EC data availability exceeded 90% in all years expect for 2006 when data were missing entirely from mid-January until the end of May. Interrogations of mean CO_2 concentrations (LI-820, Licor, Lincoln, NE, USA) in the vertical air column extending from the surface to the top of the tower with up to 7 discrete heights sampled at least 3 times every 30 min were combined to estimate the change in storage term F_s in the CO_2 mass balance. For the purpose of this paper, net ecosystem exchange of CO_2 was defined as $NEE = F_c + F_s$ knowingly neglecting both vertical and horizontal advective terms and horizontal flux divergence. All neglected terms are expected to have little impact on seasonal and annual budgets of carbon dioxide and water vapor exchange as periods with favorable for them conditions were strictly excluded when constructing aggregates. However, we acknowledge that individual 30 min estimates may have a significant stochastic error.

[62] Three methods were used for filling gaps in NEE time series resulting from either nonexistent raw data or data rejected by the quality control. For daytime conditions, two different approaches were deployed: approach 1 is light

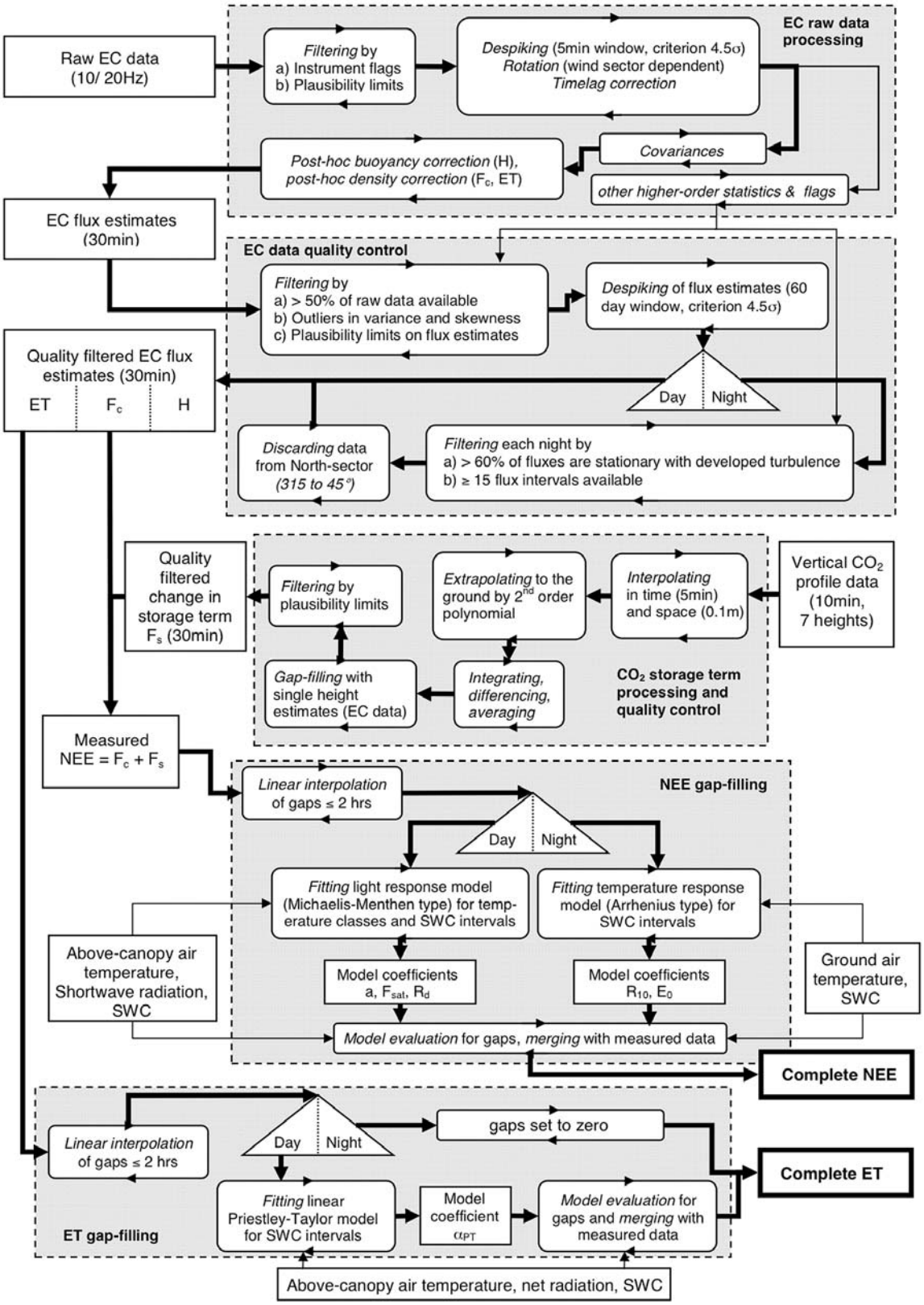

Figure A1. Comprehensive illustration of the data and workflow to derive gap-filled continuous time series of net ecosystem exchange (NEE) and evapotranspiration (ET) based on eddy covariance (EC) measurements and profile observations of mean carbon dioxide concentration at the main meteorological tower: data sets (rectangles), data processing (rectangles with rounded edges), data filters (triangles), and logical modules (gray shaded boxes). NEE is defined as the sum of turbulent EC flux (F_c) and change in storage term (F_s), H is the sensible heat flux, and SWC is the soil volumetric content.

response model (Michaelis-Menthen type model; equation (A1)) of observed and quality filtered daytime NEE estimates against global radiation (R_g) for temperature classes T_a and no differentiation of annual θ_s classes, and approach 2 is the same light response model developed for temperature classes and θ_s intervals. In case of transition time and nighttime data, three different options were pursued: option 1 is multiple linear regression of NEE estimates versus first- and second-order polynomial terms of $T_{a,1.6m}$ and θ_s (equation (A2)), option 2 is temperature response model (Arrhenius-type model; equation (A3) [*van't Hoff*, 1898]) of NEE against $T_{a,1.6m}$ without distinguishing between different θ_s intervals, and option 3 is the same temperature response model (equation (A3)) for different θ_s intervals. Transition time was defined as the 30 min interval in which sunrise or sunset occurred for each day of the year (DOY) based on calculated zenith and azimuth angles. Four intervals of θ_s were defined using the site-specific threshold of 0.3 below which the trees may experience water limitations in their carbon and water exchange rates [*Miller et al.*, 2007]: (1) DOY = 1 until $\theta_s = 0.3$, (2) $\theta_s < 0.3$ until half width of period with $\theta_s < 0.3$, (3) second half of period with $\theta_s < 0.3$ until $\theta_s = 0.3$, and (4) $\theta_s > 0.3$ until DOY = 365. Delineation of intervals using the hydroecological seasons was not pursued to prevent any bias in the resulting fluxes. We selected the combination of approach 2 and option 3 for daytime and nighttime conditions, respectively, to gap fill the observations. Gap-filled NEE time series of all approaches were composited to estimate uncertainty. NEE was partitioned into its gross components GEP and RE_{EC} by extrapolating the nighttime option 3 into daytime conditions using the above-canopy air temperature T_a instead of $T_{a,1.6m}$ to calculate daytime respiration and by calculating GEP as the residual (GEP = NEE-RE_{EC}). The following model was used for daytime conditions:

$$NEE = \frac{\alpha R_g F_{csat}}{\alpha R_g + F_{csat}} + R_{day} \tag{A1}$$

In equation (A1), α is the photon use efficiency (dimensionless), R_g the global radiation (W m^{-2}), and F_{csat} the saturation NEE flux (μmol m^{-2} s^{-1}), and R_{day} the daytime bulk respiration (μmol m^{-2} s^{-1}). For nighttime conditions, two different models were used:

$$NEE = a_0 + a_1 T_{a,1.6m} + a_2 T_{a,1.6m}^2 + a_3 \theta_s + a_4 \theta_s^2 \tag{A2}$$

In equation (A2), $a_0 \ldots a_4$ are the linear fit coefficients, $T_{a,1.6m}$ is the air temperature close to the ground at 1.6 m agl (°C), and θ_s the surface soil volumetric content integrated over the top 0.3 m (dimensionless).

$$NEE = R_{10} e^{E_0 \left(\frac{1}{283.15 - T_0} - \frac{1}{T_{a,1.6m} + 273.15 - T_0} \right)} \tag{A3}$$

In equation (A3), R_{10} is the bulk respiration value at a temperature of 10°C (μmol m^{-2} s^{-1}), E_0 a fit parameter (K), T_0 the reference temperature set to a fixed value of 227.13 (K), and $T_{a,1.6m}$ is the air temperature close to the ground at 1.6 m agl (°C).

[63] Gaps in ET time series for daytime conditions were filled using a linear model developed from regressing observed and approved data against potential evapotranspiration (PET; equation (A4) [*Priestley and Taylor*, 1972]) calculated using net radiation R_n and T_a for the same θ_s intervals used for gap filling of NEE data. Gaps in nighttime ET were set to zero.

$$ET = a \cdot pET + b = a\left(\alpha_{PT} \frac{R_n - 0.05|R_n|}{\gamma + 1} \right) + b \tag{A4}$$

In equation (A4), a (dimensionless) and b (W m^{-2}) are the slope and offset, respectively, of a linear model of observed evapotranspiration (ET (W m^{-2})) against potential evapotranspiration (PET (W m^{-2})), α_{PT} the Priestley-Taylor coefficient (dimensionless), and R_n the net radiation (W m^{-2}), and γ defined by equation (A5) with T_a being the above-canopy air temperature.

$$\gamma = 1.042 e^{0.043 T_a} - 0.4 \tag{A5}$$

Appendix B: Penman-Monteith Inversion

[64] The following Penman-Monteith flux [*Monteith*, 1965; *Penman*, 1948] provides an integrated "big leaf" approximation of evapotranspiration (ET):

$$ET = \frac{\Delta (R_n - G) + \rho_a c_p G_a (e_a^* - e_a)}{\Delta + \gamma (1 + G_a / G_c)} \tag{B1}$$

In equation (B1), Δ is the slope of the saturation vapor pressure curve (Pa K^{-1}), R_n is the net radiation (W m^{-2}), G is the ground heat flux, estimated as $0.1 \cdot R_n$, ρ_a is the density of the air (kg m^{-3}), c_p is the heat capacity of water (J kg^{-1} K^{-1}), $(e_a^* - e_a)$ is the vapor pressure deficit (Pa), γ is the psychrometric constant (Pa K^{-1}), G_c is the canopy or "ecosystem" conductance (m s^{-1}), and G_a the following aerodynamic conductance for evapotranspiration (m s^{-1}) in neutral conditions:

$$G_a = \kappa u_* \left[\ln\left(\frac{z - d_0}{z_0} \right) \right]^{-1} \tag{B2}$$

In equation (B2), κ is the von Karman constant (equal to 0.41) [*Brutsaert*, 2005], u_* is the observed friction velocity (m s^{-1}), z is the measurement height above the canopy (m), d_0 is the zero plane displacement height (m), estimated as $0.7 \cdot z_{veg}$ [*Dingman*, 2002], where z_{veg} is the canopy height (m), and z_0 is the scalar roughness length (m), assumed equal to $0.1 \cdot z_{veg}$ [*Dingman*, 2002].

[65] In this study, we solve equation (B1) for G_c using measured ET from EC data. Data in Figure 3f illustrates the maximum daily bulk ecosystem resistance (r_e) (s m^{-1}), or $1/G_c$, computed as the average of the six largest 30 min values for each day. While equation (B1) oversimplifies the complexity of vertical water transport in the soil-plant-atmosphere continuum, the resultant r_e represents the bulk ecosystem resistance to water vapor exchange into the atmosphere, a fraction of which (apart from bare soil and intercepted evaporation) is regulated by vegetative control

of water loss and carbon gain [*Jarvis*, 1976]. r_e therefore may be used as a quantitative indicator of integrated ecosystem drought stress and is an appropriate diagnostic in identifying an approximate transition between growing season limited and drought within a hydroecological year [*Pettijohn and Salvucci*, 2006; *Pettijohn et al.*, 2009].

[66] **Acknowledgments.** This research was supported by the Office of Science (BER), U.S. Department of Energy (DOE) (grant DE-FG02-06ER64318), for the AmeriFlux project "On the effects of disturbance and climate on carbon storage and the exchanges of carbon dioxide, water vapor and energy exchange of evergreen coniferous forests in the Pacific Northwest: integration of eddy flux, plant and soil measurements at a cluster of supersites." Additional support was provided by the North American Carbon Program study, "Integrating Remote Sensing, Field Observations, and Models to Understand Disturbance and Climate Effects on the Carbon Balance of the West Coast U.S.," funded by Office of Science (BER), DOE (grant DE-FG02-06ER63917). We further thank Richard Waring and Dean Vickers for many helpful discussions and comments on the manuscript and Christopher Daly for providing the high-resolution PRISM data. We also acknowledge the constructive comments of two anonymous reviewers that helped further improve the manuscript.

References

Allard, V., J. M. Ourcival, S. Rambal, R. Joffre, and A. Rocheteau (2008), Seasonal and annual variation of carbon exchange in an evergreen Mediterranean forest in southern France, *Global Change Biol.*, *14*(4), 714–725, doi:10.1111/j.1365-2486.2008.01539.x.

Andersen, C. P., D. L. Phillips, P. T. Rygiewicz, and M. J. Storm (2008), Fine root growth and mortality in different-aged ponderosa pine stands, *Can. J. For. Res.*, *38*, 1797–1806, doi:10.1139/X08-029.

Botter, G., E. Daly, A. Porporato, I. Rodriguez-Iturbe, and A. Rinaldo (2008), Probabilistic dynamics of soil nitrate: Coupling of ecohydrological and biogeochemical processes, *Water Resour. Res.*, *44*, W03416, doi:10.1029/2007WR006108.

Brooks, J. R., F. C. Meinzer, R. Coulombe, and J. Gregg (2002), Hydraulic redistribution of soil water during summer drought in two contrasting Pacific Northwest coniferous forests, *Tree Physiol.*, *22*(15–16), 1107–1117.

Brutsaert, W. (2005), *Hydrology: An Introduction*, 618 pp., Cambridge Univ. Press, Cambridge, U. K.

Curtis, P. S., P. J. Hanson, P. Bolstad, C. Barford, J. C. Randolph, H. P. Schmid, and K. B. Wilson (2002), Biometric and eddy-covariance based estimates of annual carbon storage in five eastern North American deciduous forests, *Agric. For. Meteorol.*, *113*(1–4), 3–19, doi:10.1016/S0168-1923(02)00099-0.

Daly, E., A. Porporato, and I. Rodriguez-Iturbe (2004a), Coupled dynamics of photosynthesis, transpiration, and soil water balance. Part I: Upscaling from hourly to daily level, *J. Hydrometeorol.*, *5*(3), 546–558, doi:10.1175/1525-7541(2004)005<0546:CDOPTA>2.0.CO;2.

Daly, E., A. Porporato, and I. Rodriguez-Iturbe (2004b), Coupled dynamics of photosynthesis, transpiration, and soil water balance. Part II: Stochastic analysis and ecohydrological significance, *J. Hydrometeorol.*, *5*(3), 559–566, doi:10.1175/1525-7541(2004)005<0559:CDOPTA>2.0.CO;2.

Dingman, S. L. (2002), *Physical Hydrology*, Prentice Hall, Upper Saddle River, N. J.

Elias, T. S. (1980), *The Complete Trees of North America*, Van Nostrand Reinhold, New York.

Falge, E., et al. (2002), Seasonality of ecosystem respiration and gross primary production as derived from FLUXNET measurements, *Agric. For. Meteorol.*, *113*(1–4), 53–74, doi:10.1016/S0168-1923(02)00102-8.

Falk, M., S. Wharton, M. Schroeder, S. Ustin, and K. T. Paw U (2008), Flux partitioning in an old-growth forest: Seasonal and interannual dynamics, *Tree Physiol.*, *28*(4), 509–520.

Foken, T., and B. Wichura (1996), Tools for quality assessment of surface-based flux measurements, *Agric. For. Meteorol.*, *78*(1–2), 83–105, doi:10.1016/0168-1923(95)02248-1.

Foken, T., M. Göckede, M. Mauder, L. Mahrt, B. D. Amiro, and J. W. Munger (2004), Post-field data quality control, in *Handbook of Micrometeorology: A Guide for Surface Flux Measurements*, edited by X. Lee, W. J. Massman, and B. Law, pp. 181–208, Kluwer Acad., Dordrecht, Netherlands.

Gough, C. M., C. S. Vogel, H. P. Schmid, H. B. Su, and P. S. Curtis (2008), Multi-year convergence of biometric and meteorological estimates of forest carbon storage, *Agric. For. Meteorol.*, *148*(2), 158–170, doi:10.1016/j.agrformet.2007.08.004.

Granier, A. (1987), Sap flow measurements in Douglas-fir tree trunks by means of a new thermal method, *Ann. Sci. For.*, *44*(1), 1–14, doi:10.1051/forest:19870101.

Granier, A. (2007), Evidence for soil water control on carbon and water dynamics in European forests during the extremely dry year: 2003, *Agric. For. Meteorol.*, *143*(1–2), 123–145, doi:10.1016/j.agrformet.2006.12.004.

Grunzweig, J. M., T. Lin, E. Rotenberg, A. Schwartz, and D. Yakir (2003), Carbon sequestration in arid-land forest, *Global Change Biol.*, *9*(5), 791–799, doi:10.1046/j.1365-2486.2003.00612.x.

Hale, M. G., and D. M. Orcutt (1987), *The Physiology of Plants Under Stress*, 683 pp., John Wiley, New York.

Hargrove, W. W., F. M. Hoffman, and B. E. Law (2003), New analysis reveals representativeness of the AmeriFlux network, *Eos Trans. AGU*, *84*(48), doi:10.1029/2003EO480001.

Irvine, J., and B. E. Law (2002), Contrasting soil respiration in young and old-growth ponderosa pine forests, *Global Change Biol.*, *8*(12), 1183–1194, doi:10.1046/j.1365-2486.2002.00544.x.

Irvine, J., B. E. Law, M. R. Kurpius, P. M. Anthoni, D. Moore, and P. A. Schwarz (2004), Age-related changes in ecosystem structure and function and effects on water and carbon exchange in ponderosa pine, *Tree Physiol.*, *24*(7), 753–763.

Irvine, J., B. E. Law, and K. A. Hibbard (2007), Postfire carbon pools and fluxes in semiarid ponderosa pine in central Oregon, *Global Change Biol.*, *13*(8), 1748–1760, doi:10.1111/j.1365-2486.2007.01368.x.

Irvine, J., B. E. Law, J. G. Martin, and D. Vickers (2008), Interannual variation in soil CO_2 efflux and the response of root respiration to climate and canopy gas exchange in mature ponderosa pine, *Global Change Biol.*, *14*(12), 2848–2859, doi:10.1111/j.1365-2486.2008.01682.x.

Jarvis, P. G. (1976), The interpretation of the variations in leaf water potential and stomatal conductance found in canopies in the field, *Philos. Trans. R. Soc. London, Ser. B*, *273*, 593–610.

Jassal, R. S., T. A. Black, T. B. Cai, K. Morgenstern, Z. Li, D. Gaumont-Guay, and Z. Nesic (2007), Components of ecosystem respiration and an estimate of net primary productivity of an intermediate-aged Douglas-fir stand, *Agric. For. Meteorol.*, *144*(1–2), 44–57, doi:10.1016/j.agrformet.2007.01.011.

Kenney, B. C. (1982), Beware of spurious self-correlations!, *Water Resour. Res.*, *18*, 1041–1048.

Krishnan, P., T. A. Black, N. J. Grant, A. G. Barr, E. T. H. Hogg, R. S. Jassal, and K. Morgenstern (2006), Impact of changing soil moisture distribution on net ecosystem productivity of a boreal aspen forest during and following drought, *Agric. For. Meteorol.*, *139*(3–4), 208–223, doi:10.1016/j.agrformet.2006.07.002.

Krishnan, P., T. A. Black, A. G. Barr, N. J. Grant, D. Gaumont-Guay, and Z. Nesic (2008), Factors controlling the interannual variability in the carbon balance of a southern boreal black spruce forest, *J. Geophys. Res.*, *113*, D09109, doi:10.1029/2007JD008965.

Lagergren, F., A. Lindroth, E. Dellwik, A. Ibrom, H. Lankreijer, S. Launiainen, M. Molder, P. Kolari, K. Pilegaard, and T. Vesala (2008), Biophysical controls on CO_2 fluxes of three northern forests based on long-term eddy covariance data, *Tellus, Ser. B*, *60*(2), 143–152.

Laio, F., A. Porporato, C. P. Fernandez-Illescas, and I. Rodriguez-Iturbe (2001), Plants in water-controlled ecosystems: Active role in hydrologic processes and response to water stress—IV. Discussion of real cases, *Adv. Water Resour.*, *24*(7), 745–762, doi:10.1016/S0309-1708(01)00007-0.

Law, B. E., and R. H. Waring (1994), Combining remote sensing and climatic data to estimate net primary production across Oregon, *Ecol. Appl.*, *4*(4), 717–728, doi:10.2307/1942002.

Law, B. E., M. G. Ryan, and P. M. Anthoni (1999), Seasonal and annual respiration of a ponderosa pine ecosystem, *Global Change Biol.*, *5*(2), 169–182, doi:10.1046/j.1365-2486.1999.00214.x.

Law, B. E., M. Williams, P. M. Anthoni, D. D. Baldocchi, and M. H. Unsworth (2000), Measuring and modelling seasonal variation of carbon dioxide and water vapour exchange of a Pinus ponderosa forest subject to soil water deficit, *Global Change Biol.*, *6*(6), 613–630, doi:10.1046/j.1365-2486.2000.00339.x.

Law, B. E., F. M. Kelliher, D. D. Baldocchi, P. M. Anthoni, J. Irvine, D. Moore, and S. Van Tuyl (2001a), Spatial and temporal variation in respiration in a young ponderosa pine forest during a summer drought, *Agric. For. Meteorol.*, *110*(1), 27–43, doi:10.1016/S0168-1923(01)00279-9.

Law, B. E., P. E. Thornton, J. Irvine, P. M. Anthoni, and S. Van Tuyl (2001b), Carbon storage and fluxes in ponderosa pine forests at different developmental stages, *Global Change Biol.*, *7*(7), 755–777, doi:10.1046/j.1354-1013.2001.00439.x.

Law, B. E., et al. (2002), Environmental controls over carbon dioxide and water vapor exchange of terrestrial vegetation, *Agric. For. Meteorol.*, *113*(1–4), 97–120, doi:10.1016/S0168-1923(02)00104-1.

Luyssaert, S., et al. (2007), Photosynthesis drives anomalies in net carbon-exchange of pine forests at different latitudes, *Global Change Biol.*, *13*(10), 2110–2127, doi:10.1111/j.1365-2486.2007.01432.x.

Ma, S. Y., D. D. Baldocchi, L. K. Xu, and T. Hehn (2007), Inter-annual variability in carbon dioxide exchange of an oak/grass savanna and open grassland in California, *Agric. For. Meteorol.*, *147*(3–4), 157–171, doi:10.1016/j.agrformet.2007.07.008.

Mantua, N. J., S. R. Hare, Y. Zhang, J. M. Wallace, and R. C. Francis (1997), A Pacific interdecadal climate oscillation with impacts on salmon production, *Bull. Am. Meteorol. Soc.*, *78*(6), 1069–1079, doi:10.1175/1520-0477(1997)078<1069:APICOW>2.0.CO;2.

Maseyk, K., J. M. Grunzweig, E. Rotenberg, and D. Yakir (2008), Respiration acclimation contributes to high carbon-use efficiency in a seasonally dry pine forest, *Global Change Biol.*, *14*(7), 1553–1567, doi:10.1111/j.1365-2486.2008.01604.x.

Miller, G. R., D. D. Baldocchi, B. E. Law, and T. Meyers (2007), An analysis of soil moisture dynamics using multi-year data from a network of micrometeorological observation sites, *Adv. Water Resour.*, *30*(5), 1065–1081, doi:10.1016/j.advwatres.2006.10.002.

Monteith, J. L. (1965), Evaporation and environment, *Symp. Soc. Exp. Biol.*, *19*, 205–234.

Nilsen, E. T., and D. M. Orcutt (1996), *Physiology of Plants Under Stress: Abiotic Factors*, 689 pp., John Wiley, New York.

Penman, H. L. (1948), Natural evaporation from open water, bare soil and grass, *Philos. Trans. R. Soc. London, Ser. A*, *193*, 120–145.

Pereira, J. S., et al. (2007), Net ecosystem carbon exchange in three contrasting Mediterranean ecosystems—The effect of drought, *Biogeosciences*, *4*(5), 791–802.

Pettijohn, J. C., and G. D. Salvucci (2006), Impact of an unstressed canopy conductance on the Bouchet-Morton complementary relationship, *Water Resour. Res.*, *42*, W09418, doi:10.1029/2005WR004385.

Pettijohn, J. C., G. D. Salvucci, N. G. Phillips, and M. J. Daley (2009), Mechanisms of moisture stress in a mid-latitude temperate forest: Implications for feedforward and feedback controls from an irrigation experiment, *Ecol. Modell.*, *220*(7), 968–978, doi:10.1016/j.ecolmodel.2008.12.020.

Porporato, A., F. Laio, L. Ridolfi, and I. Rodriguez-Iturbe (2001), Plants in water-controlled ecosystems: Active role in hydrologic processes and response to water stress—III. Vegetation water stress, *Adv. Water Resour.*, *24*(7), 725–744, doi:10.1016/S0309-1708(01)00006-9.

Powell, D. S., J. L. Faulkner, D. R. Darr, Z. Zhu, and D. W. MacCleery (1993), Forest resources of the United States, 1992, *Gen. Tech. Rep. RM-234*, U.S. Dep. of Agric. For. Serv., Rocky Mt. For. and Range Exp. Stn., Fort Collins, Colo.

Priestley, C. H. B., and J. R. Taylor (1972), On the assessment of surface heat flux and evaporation using large-scale parameters, *Mon. Weather Rev.*, *100*, 81–82, doi:10.1175/1520-0493(1972)100<0081:OTAOSH>2.3.CO;2.

Reichstein, M., J. D. Tenhunen, O. Roupsard, J. M. Ourcival, S. Rambal, F. Miglietta, A. Peressotti, M. Pecchiari, G. Tirone, and R. Valentini (2002), Severe drought effects on ecosystem CO_2 and H_2O fluxes at three Mediterranean evergreen sites: Revision of current hypotheses?, *Global Change Biol.*, *8*(10), 999–1017, doi:10.1046/j.1365-2486.2002.00530.x.

Reichstein, M., et al. (2007), Reduction of ecosystem productivity and respiration during the European summer 2003 climate anomaly: A joint flux tower, remote sensing and modelling analysis, *Global Change Biol.*, *13*(3), 634–651, doi:10.1111/j.1365-2486.2006.01224.x.

Rodriguez-Iturbe, I., and A. Porporato (2004), *Ecohydrology of Water-Controlled Ecosystems: Soil Moisture and Plant Dynamics*, 442 pp., Cambridge Univ. Press, Cambridge, U. K.

Ryu, Y., D. D. Baldocchi, S. Ma, and T. Hehn (2008), Interannual variability of evapotranspiration and energy exchange over an annual grassland in California, *J. Geophys. Res.*, *113*, D09104, doi:10.1029/2007JD009263.

Schwarz, P. A., B. E. Law, M. Williams, J. Irvine, M. Kurpius, and D. Moore (2004), Climatic versus biotic constraints on carbon and water fluxes in seasonally drought-affected ponderosa pine ecosystems, *Global Biogeochem. Cycles*, *18*, GB4007, doi:10.1029/2004GB002234.

Thomas, C., and T. Foken (2002), Re-evaluation of integral turbulence characteristics and their parameterisations, paper presented at 15th Symposium on Boundary Layers and Turbulence, Am. Meteorol. Soc., Wageningen, Netherlands.

Thornton, P. E., S. W. Running, and M. A. White (1997), Generating surfaces of daily meteorological variables over large regions of complex terrain, *J. Hydrol.*, *190*, 214–251, doi:10.1016/S0022-1694(96)03128-9.

Tirone, G., S. Dore, G. Matteucci, S. Greco, and R. Valentini (2003), Evergreen Mediterranean forests: Carbon and water fluxes, balances, ecological and ecophysiological determinants, in *Ecological Studies*, vol. 163, *Fluxes of Carbon, Water and Energy of European Forests*, edited by R. Valentini, pp. 125–149, Springer, New York.

Urbanski, S., C. Barford, S. Wofsy, C. Kucharik, E. Pyle, J. Budney, K. McKain, D. Fitzjarrald, M. Czikowsky, and J. W. Munger (2007), Factors controlling CO_2 exchange on timescales from hourly to decadal at Harvard Forest, *J. Geophys. Res.*, *112*, G02020, doi:10.1029/2006JG000293.

Valentini, R., et al. (2000), Respiration as the main determinant of carbon balance in European forests, *Nature*, *404*(6780), 861–865, doi:10.1038/35009084.

van't Hoff, J. H. (1898), *Lectures on Theoretical and Physical Chemistry. Part I, Chemical Dynamics* (translated by R. A. Lehfeldt), pp. 224–229, Edward Arnold, London.

Vickers, D., and L. Mahrt (1997), Quality control and flux sampling problems for tower and aircraft data, *J. Atmos. Oceanic Technol.*, *14*, 512–526, doi:10.1175/1520-0426(1997)014<0512:QCAFSP>2.0.CO;2.

Vickers, D., C. Thomas, and B. E. Law (2009a), Random and systematic CO_2 flux sampling errors for tower measurements over forests in the convective boundary layer, *Agric. For. Meteorol.*, *149*(1), 73–83, doi:10.1016/j.agrformet.2008.07.005.

Vickers, D., C. K. Thomas, J. G. Martin, and B. Law (2009b), Self-correlation between assimilation and respiration resulting from flux partitioning of eddy-covariance CO_2 fluxes, *Agric. For. Meteorol.*, *149*(9), 1552–1555, doi:10.1016/j.agrformet.2009.03.009.

Waring, R. H., and S. W. Running (2007), *Forest Ecosystems: Analysis at Multiple Scales*, 420 pp., Elsevier, Burlington, Mass.

Webb, E. K., G. I. Pearman, and R. Leuning (1980), Correction of the flux measurements for density effects due to heat and water vapour transfer, *Q. J. R. Meteorol. Soc.*, *106*, 85–100, doi:10.1002/qj.49710644707.

Xu, L. K., and D. D. Baldocchi (2004), Seasonal variation in carbon dioxide exchange over a Mediterranean annual grassland in California, *Agric. For. Meteorol.*, *123*(1–2), 79–96, doi:10.1016/j.agrformet.2003.10.004.

Yuan, F. M., M. A. Arain, A. G. Barr, T. A. Black, C. P. A. Bourque, C. Coursolle, H. A. Margolis, J. H. McCaughey, and S. C. Wofsy (2008), Modeling analysis of primary controls on net ecosystem productivity of seven boreal and temperate coniferous forests across a continental transect, *Global Change Biol.*, *14*(8), 1765–1784, doi:10.1111/j.1365-2486.2008.01612.x.

Zhang, Y., J. M. Wallace, and D. S. Battisti (1997), ENSO-like interdecadal variability: 1900–93, *J. Clim.*, *10*(5), 1004–1020, doi:10.1175/1520-0442(1997)010<1004:ELIV>2.0.CO;2.

K. J. Davis, J. Irvine, B. E. Law, J. G. Martin, and J. C. Pettijohn, Department of Forest Ecosystems and Society, College of Forestry, Oregon State University, Corvallis, OR 97331-5752, USA.

C. K. Thomas, College of Oceanic and Atmospheric Sciences, Oregon State University, 104 COAS Administration Bldg., Corvallis, OR 97331-5503, USA. (chthomas@coas.oregonstate.edu)